Recent Improvements to Resolved and Parameterized Gravity-Wave Dynamics in NAVGEM, the Navy's Global Numerical Weather Prediction System

Steve Eckermann[1], Jun Ma[2], Dave Broutman[2], Harold Knight[2], James D. Doyle[3], Kevin C. Viner[3], John P. McCormack[1], Timothy R. Whitcomb[3], Timothy F. Hogan[3], Karl W. Hoppel[4], David D. Kuhl[4], Benjamin C. Ruston[3], Nancy L. Baker[3], Ronald B. Smith[5], David C. Fritts[6], Michael J. Taylor[7], Andreas Dörnbrack[8] , P.-D.Pautet[7] , B. P. Williams[6] and K. Bossert[6]

1. *Space Science Division, Naval Research Laboratory, Washington, DC*
2. *Computational Physics, Inc., Springfield, Virginia*
3. *Marine Meteorology Division, Naval Research Laboratory, Monterey, CA*
4. *Remote Sensing Division, Naval Research Laboratory, Washington, DC*
5. *Department of Geology and Geophysics, Yale University, New Haven CT*
6. *GATS, Inc., Boulder CO*
7. *Department of Physics, Utah State University, Logan UT*
8. *German Aerospace Center (DLR), Oberpfaffenhofen, Germany*

This work is/was supported by:

- *The Chief of Naval Research (CNR) through the NRL base 6.1 and 6.2 research program*
- *The Office of Naval Research (ONR)*
- *The National Science Foundation*
- *The Oceanographer of the Navy*

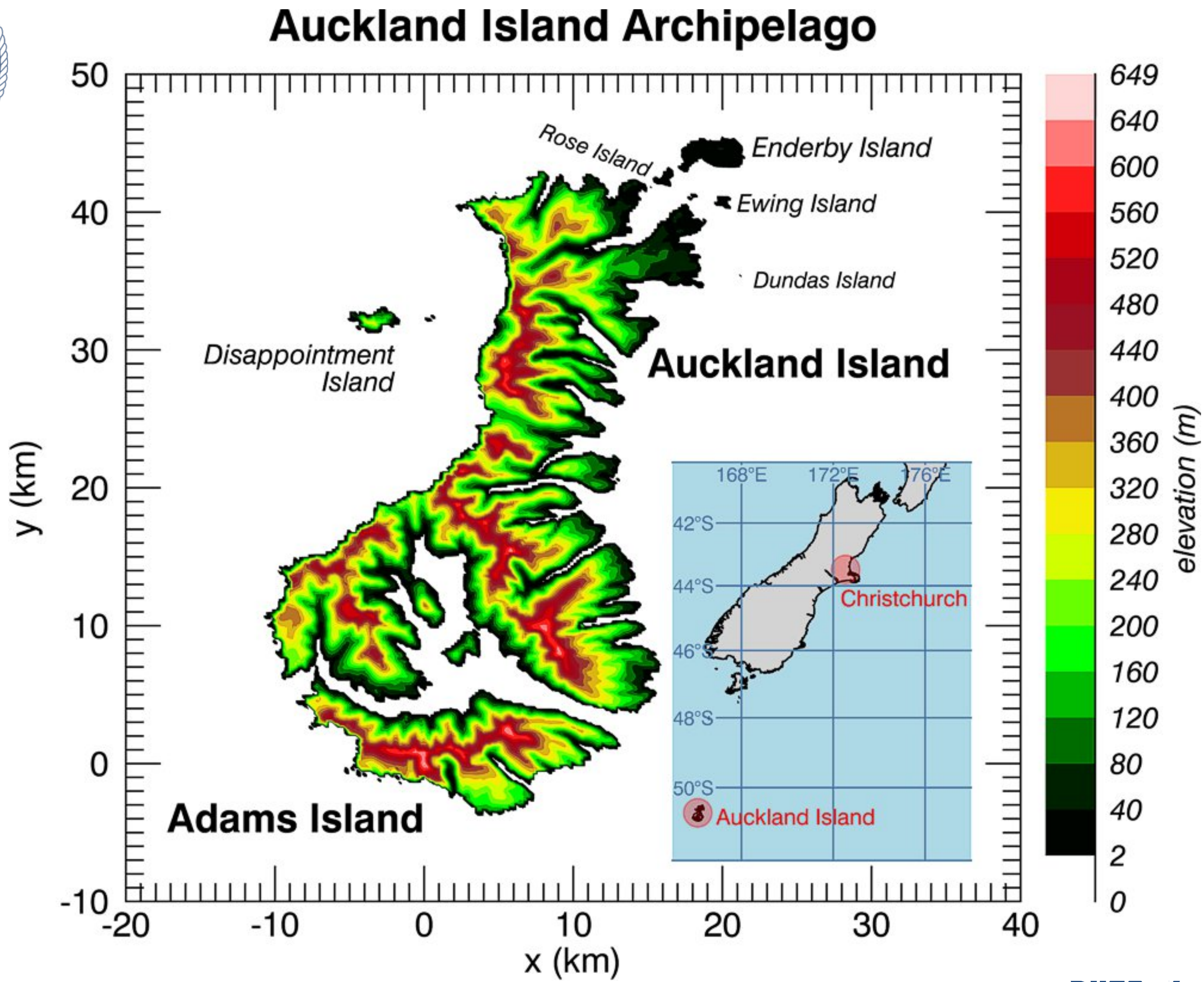
Auckland Island Archipelago
Rose Island
Enderby Island
Ewing Island
Dundas Island
Disappointment Island
Auckland Island
Adams Island
168°E
172°E
176°E
42°S
44°S
46°S
48°S
50°S
Christchurch
Auckland Island
y (km)
x (km)
elevation (m)
649
640
600
560
520
480
440
400
360
320
280
240
200
160
120
80
40
2
0

DEEPWAVE Research Flight 23
14 July 2014

Outbound RF23 Flight Leg

AMTM OH Airglow Imagery (Pautet et al. JGR, 2016)

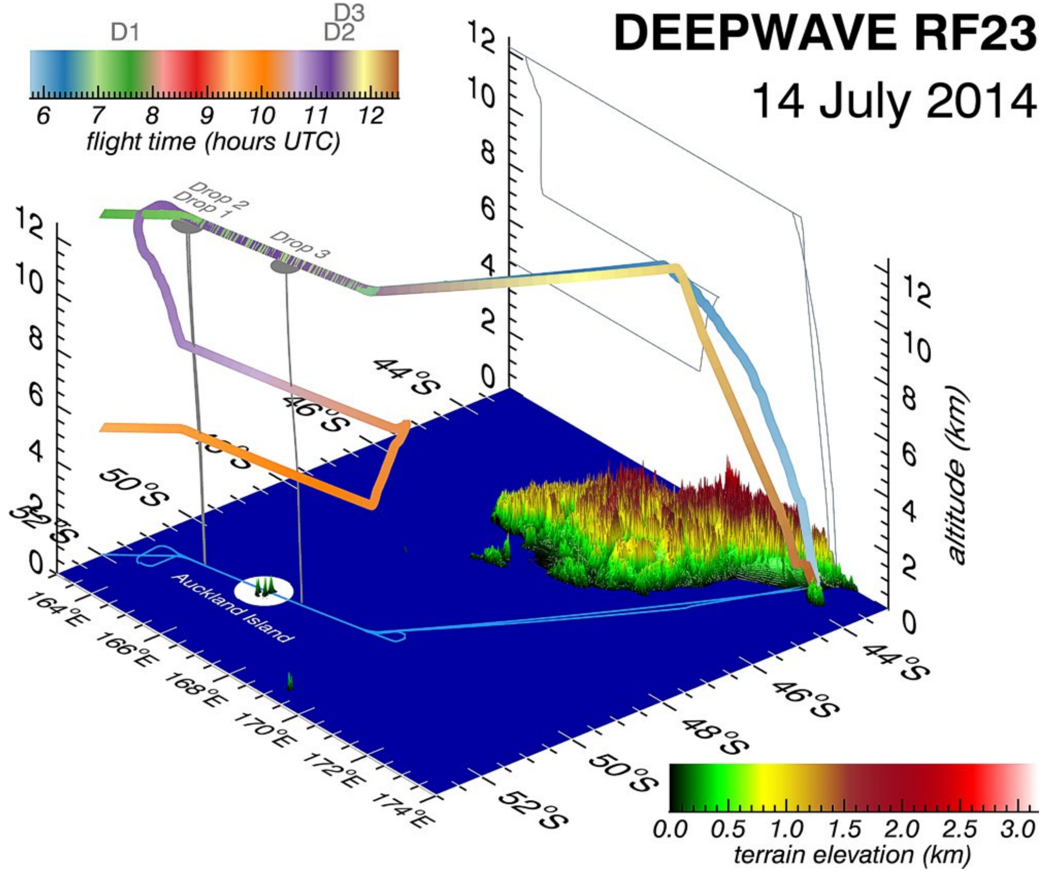

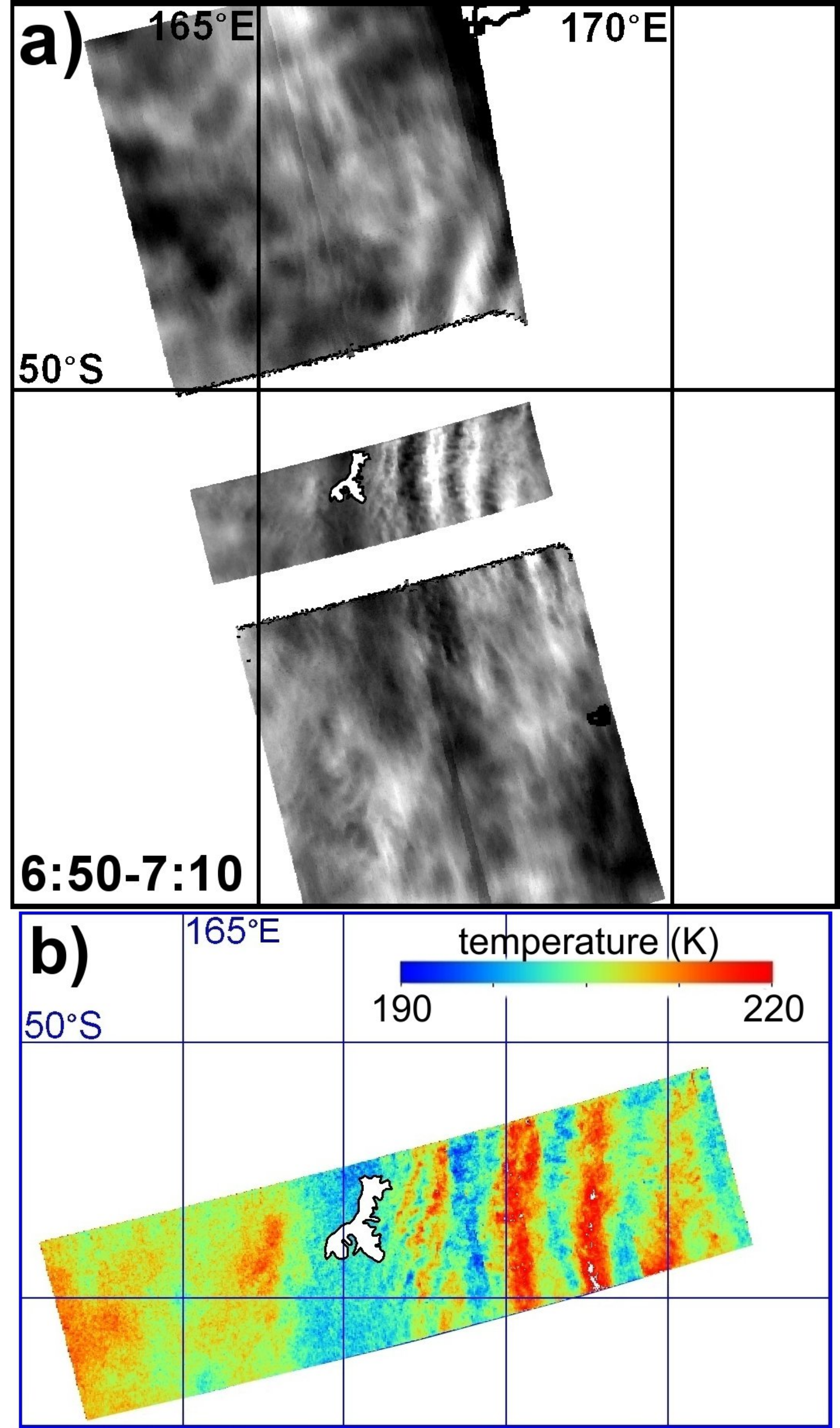

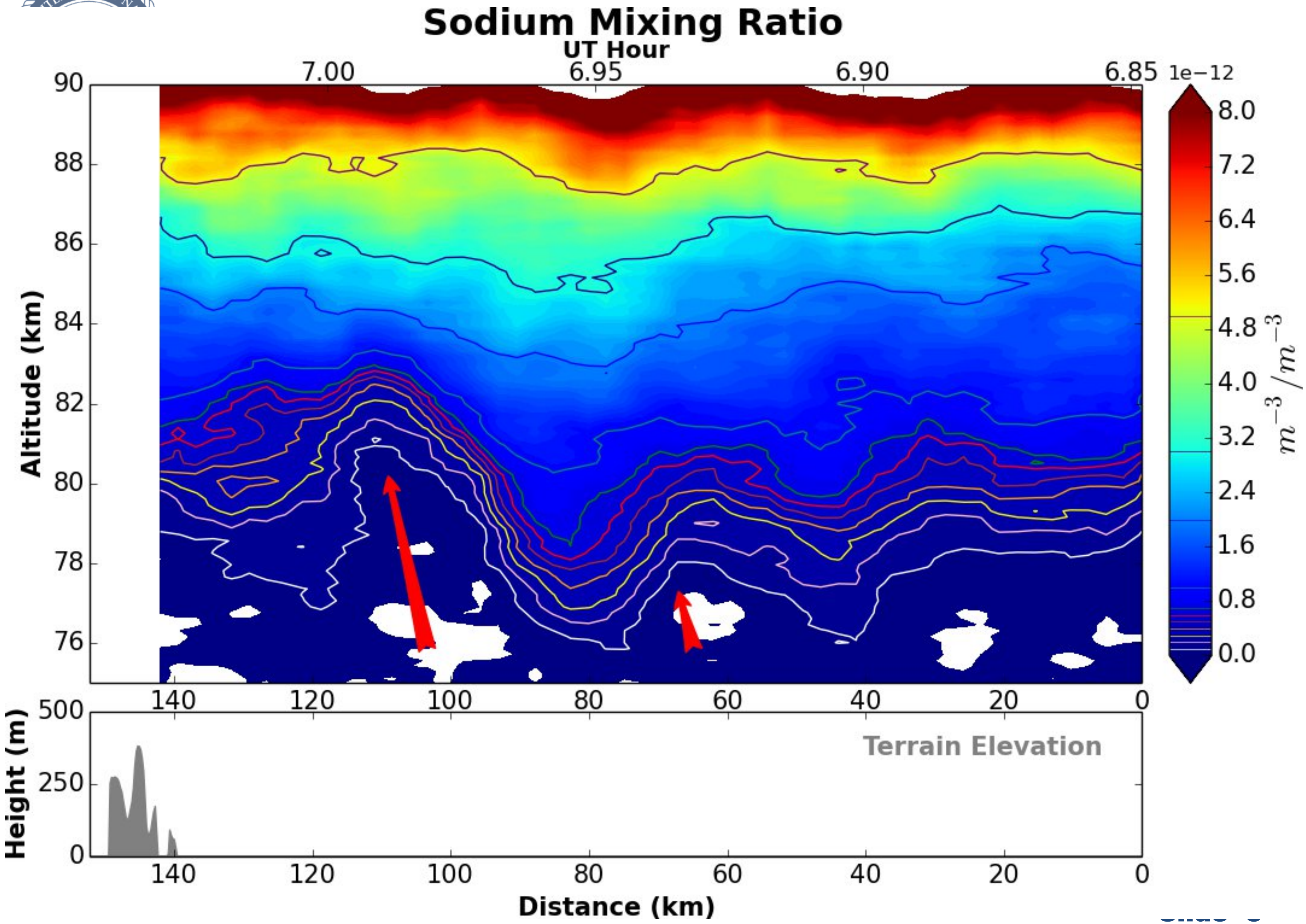

Sodium Mixing Ratio
UT Hour
7.00
6.95
6.90
6.85
1e−12
90
88
86
84
82
80
78
76
Altitude (km)
8.0
7.2
6.4
5.6
4.8
4.0
3.2
2.4
1.6
0.8
0.0
m^{-3}/m^{-3}
140
120
100
80
60
40
20
0
500
250
0
Height (m)
Terrain Elevation
Distance (km)

Linear Three-Dimensional Fourier-Ray Gravity-Wave Model

$$\hat{\omega}(k,l,z) = -kU(z) - lV(z) \qquad k_h^2 = k^2 + l^2 \qquad s(k,l) = -\mathrm{sgn}\left[\hat{\omega}(k,l,0)\right]$$

$$m(k,l,z) = s\left[\frac{(k^2+l^2)(N^2-\epsilon_n\hat{\omega}^2)}{\hat{\omega}^2-\epsilon_r f^2}\right]^{1/2}$$

ε_n = 1: nonhydrostatic solutions
ε_n = 0: hydrostatic solutions

$$X(x,y,z) = \iint_{-\infty}^{\infty} S(k,l,z)\tilde{X}(k,l,z)e^{\imath(kx+ly)}\,dk\,dl\,.$$

$$\hat{\eta}(k,l,z) = \hat{h}(k,l)\left[\frac{c_{gz}(k,l,0)\hat{\omega}(k,l,z)\rho(0)\mathcal{P}(0)N^2(0)}{c_{gz}(k,l,z)\hat{\omega}(k,l,0)\rho(z)\mathcal{P}(z)N^2(z)}\right]^{1/2} e^{\imath\int_0^z m(k,l,\tilde{z})d\tilde{z}}$$

$$c_{gz}(k,l,z) = \frac{\partial\hat{\omega}}{\partial m} = \frac{-m(\hat{\omega}^2-\epsilon_r f^2)}{\hat{\omega}[\epsilon_n(k^2+l^2)+m^2]}$$

$$t_{prop}(k,l,z) = \int_0^z c_{gz}^{-1}(k,l,z')dz'$$

$$S_{prop}(k,l,z,t) = \begin{cases} 1 & z \le z_c(k,l,t)\ [t_{prop}(k,l,z) \le t], \\ 0 & z > z_c(k,l,t)\ [t_{prop}(k,l,z) > t], \end{cases}$$

NAVGEM Reanalyses for DEEPWAVE Austral Winter (T119L74 & T425L74)

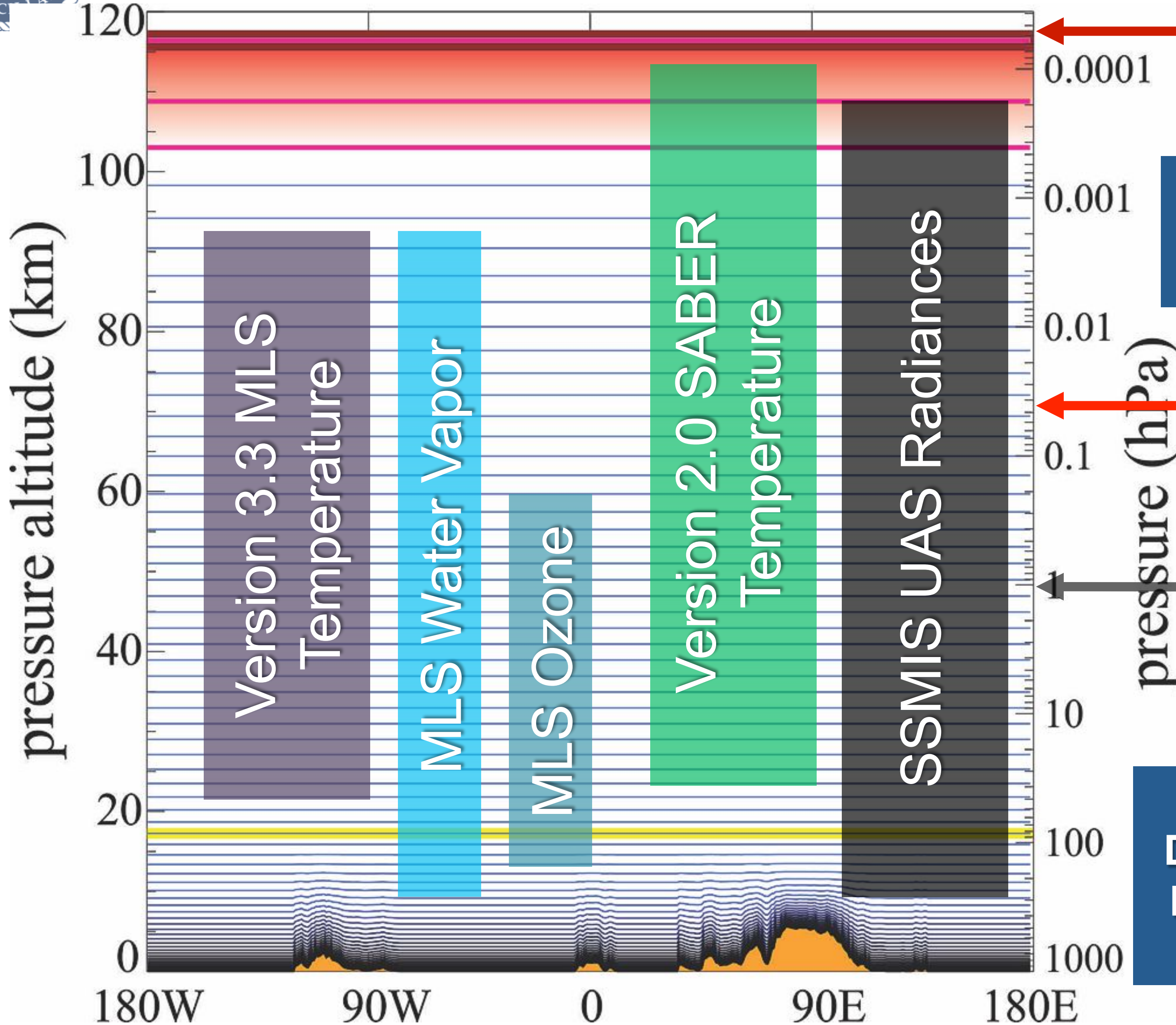

Reanalysis Upper Boundary
p_{top}=6x10^{-5} hPa

Both Pure 4DVAR & Hybrid Ensemble 4DVAR Reanalyses

Current Operational Upper Boundary

Top Data Level Assimilated Operationally

The NGV Dropwindsonde Data Were Also Assimilated

Modeled Wavefield Response in MLT Airglow 0700 UTC

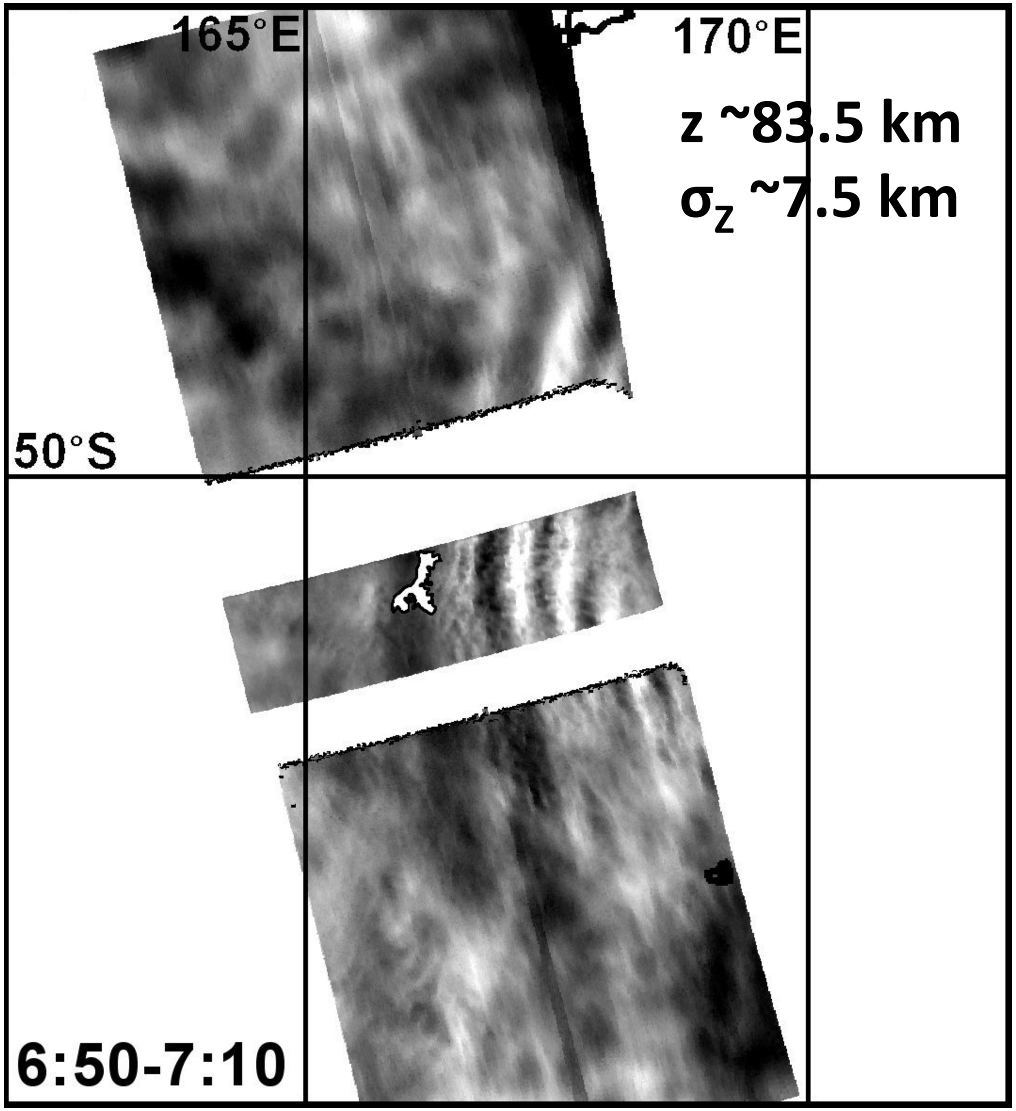

$$T'_{AG}(x,y) = \int I(z')T'(x,y,z')dz' \Big/ \int I(z')dz'$$

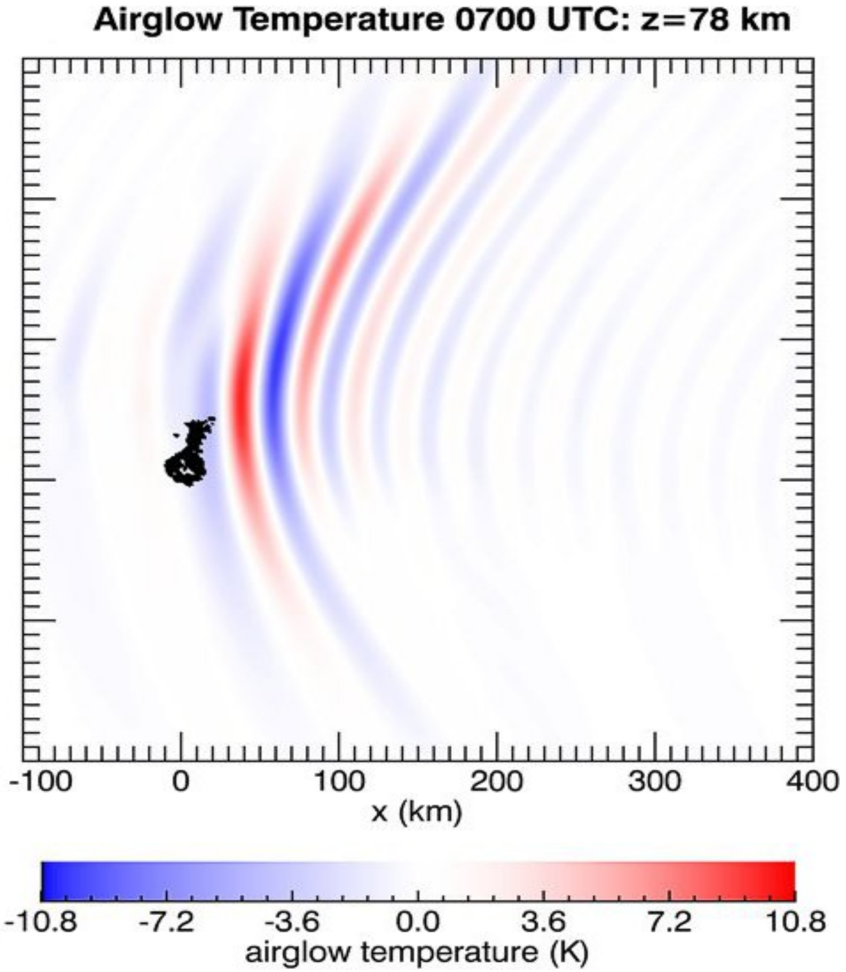

Maximum Wavefield Steepness in Fourier-Ray "Hindcasts"

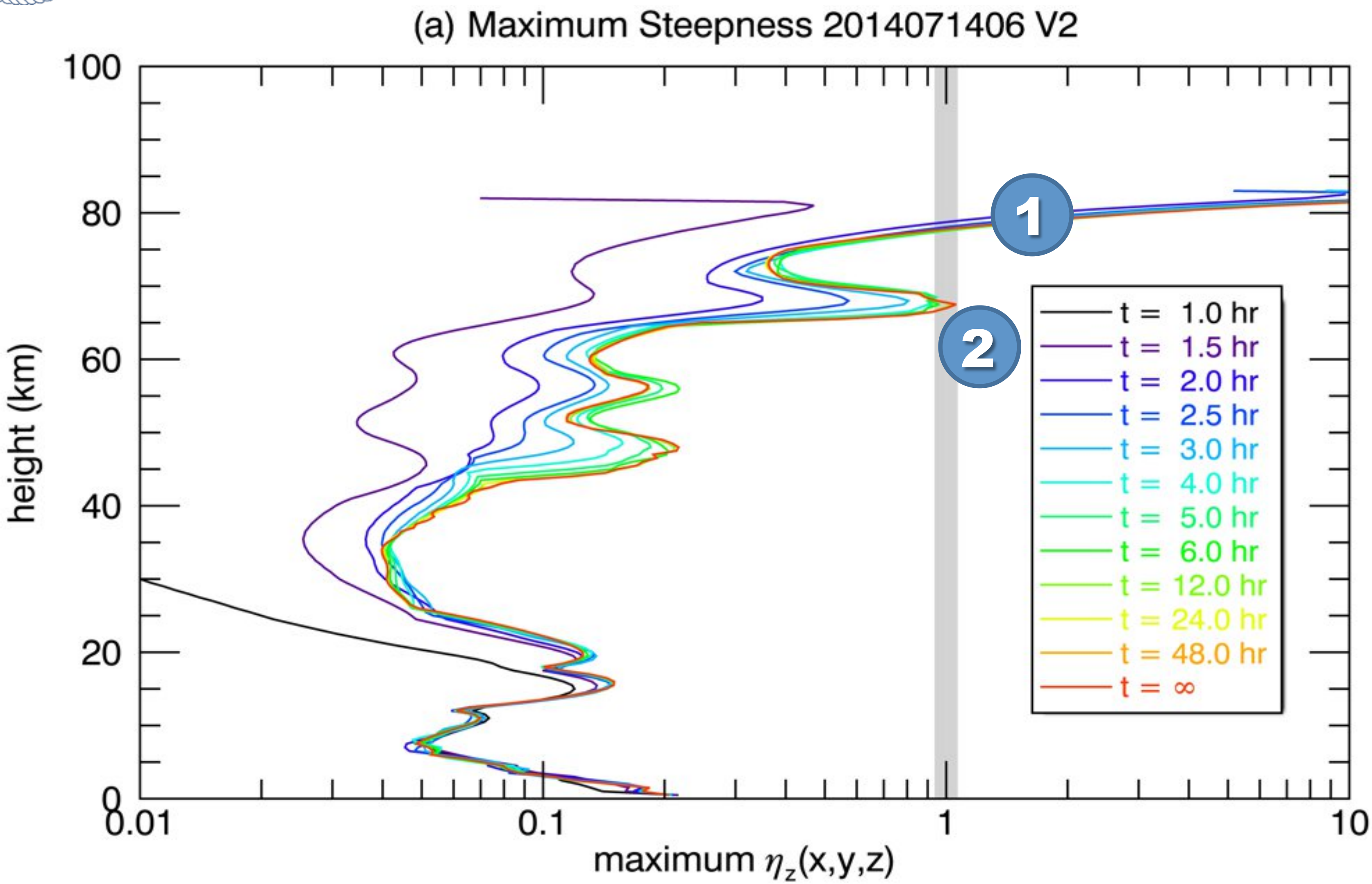

Linear Model Succeeds

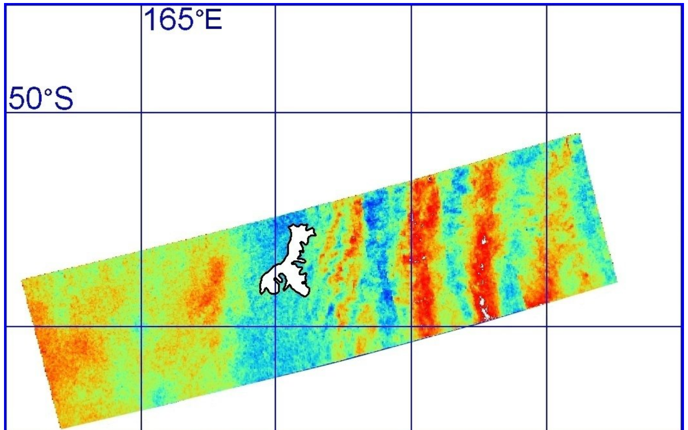

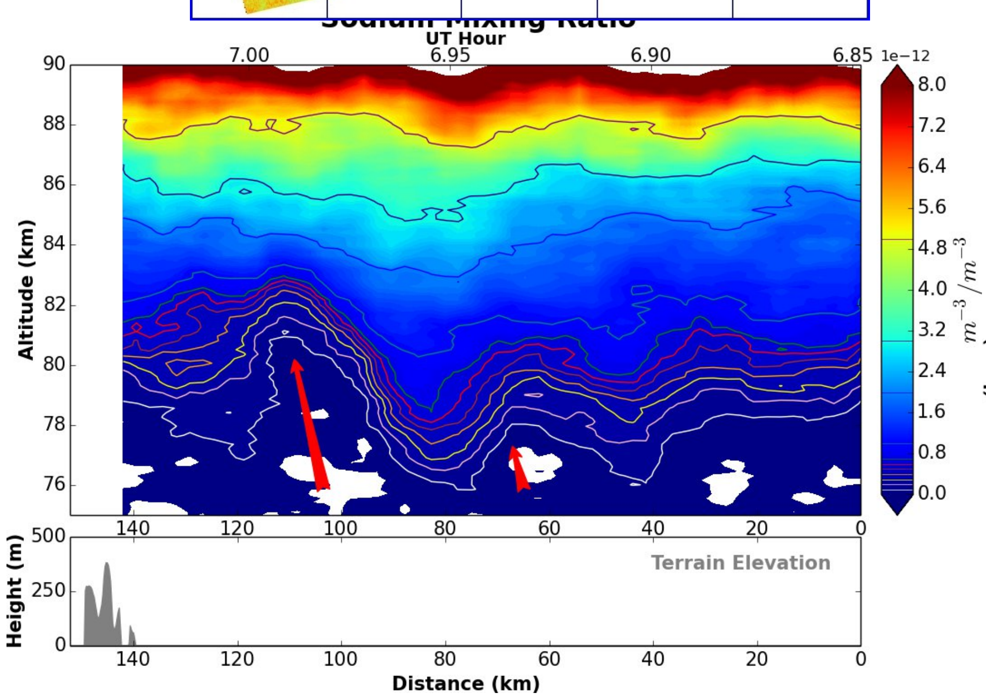

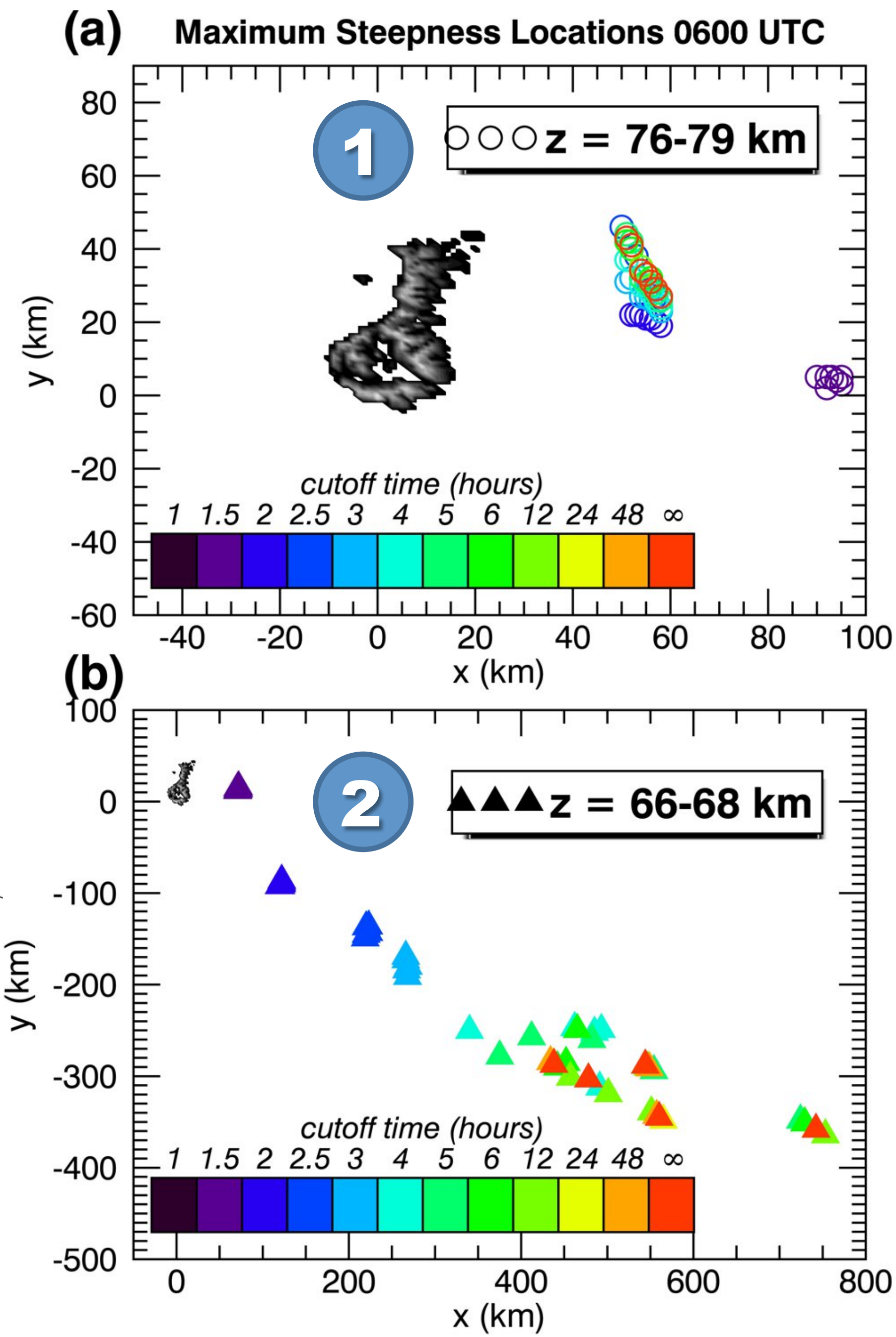

Inbound RF23 Flight Legs

DEEPWAVE RF23

14 July 2014

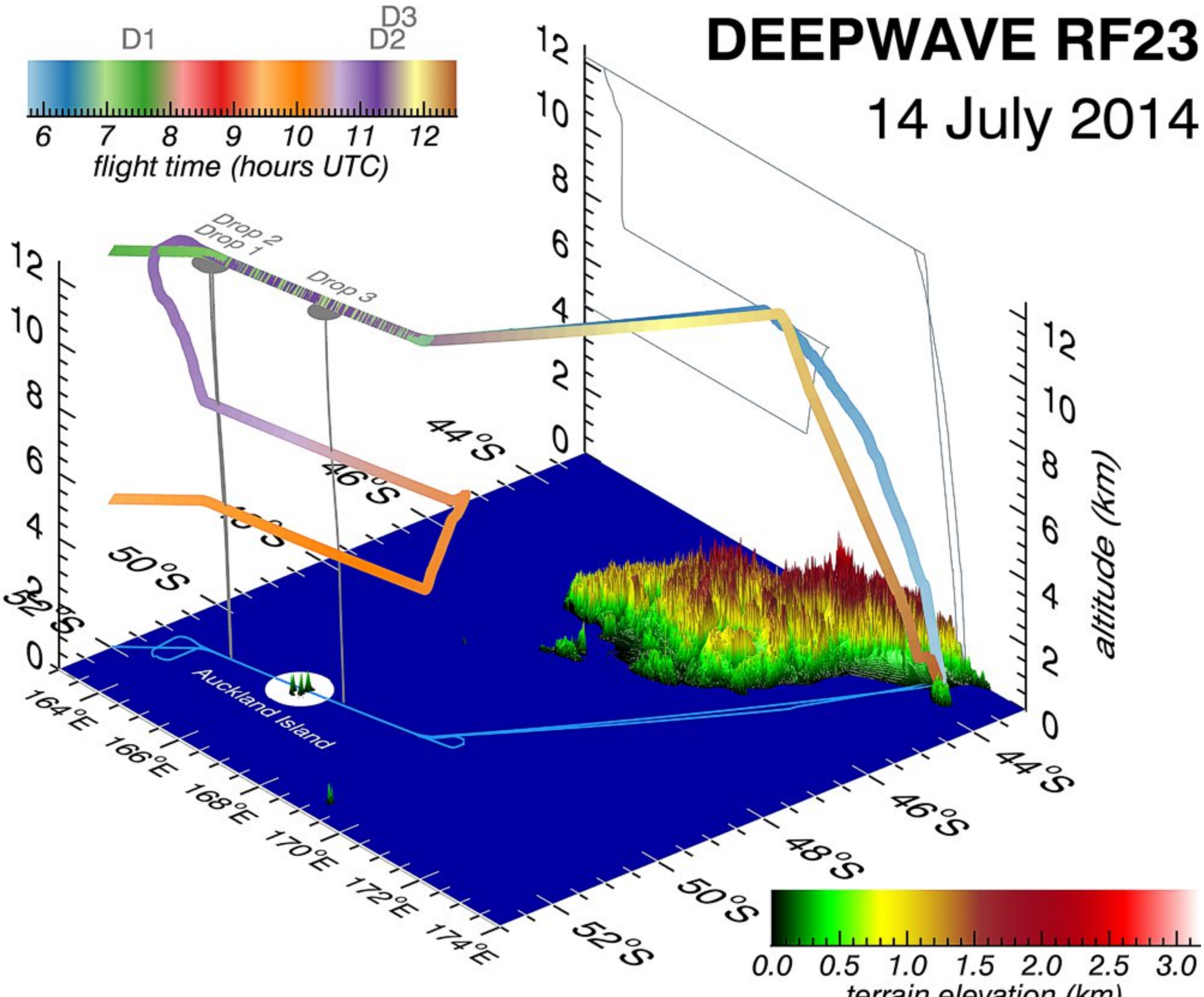

Inbound AMTM Imagery

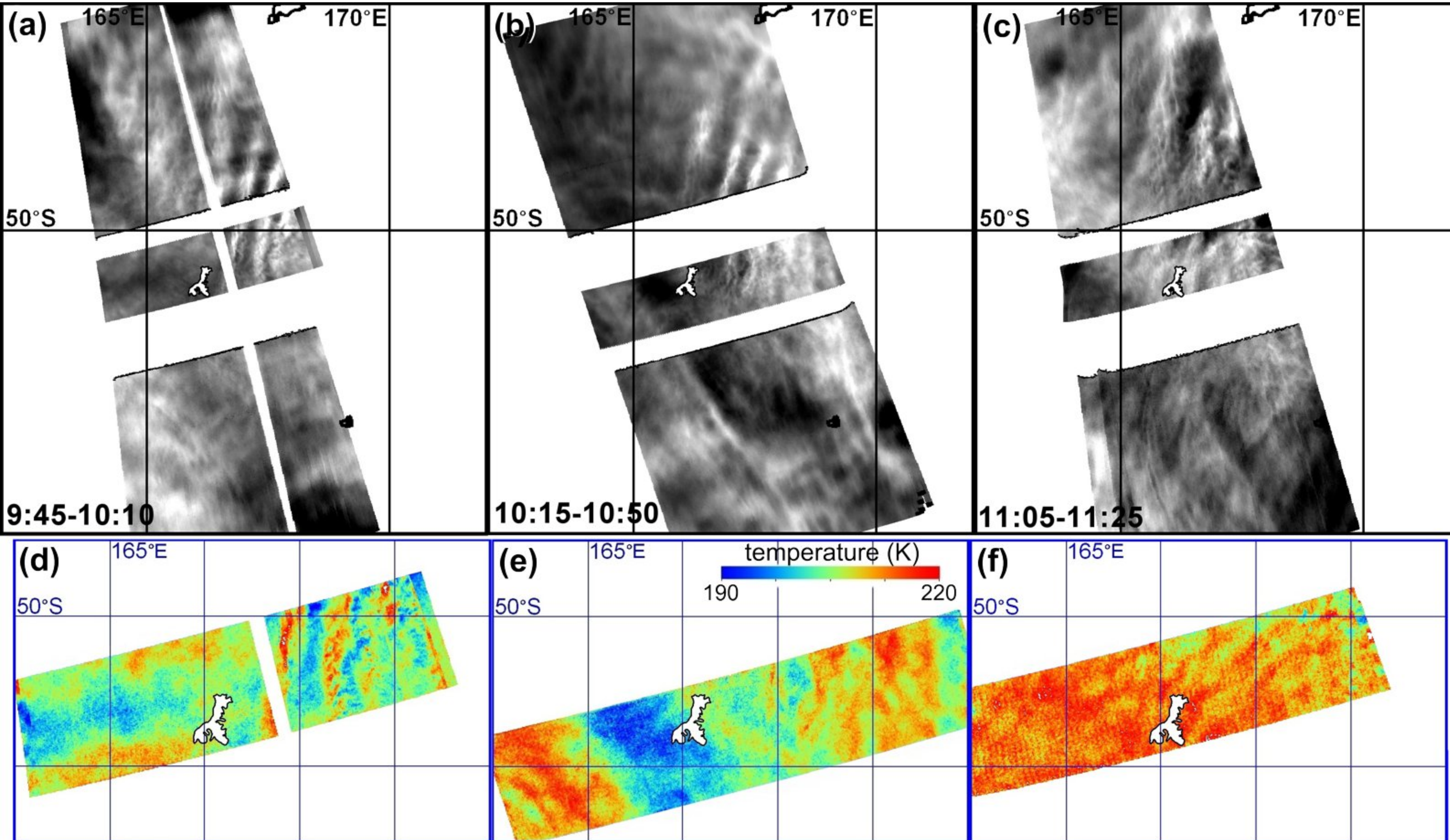

Upstream Reanalysis Winds

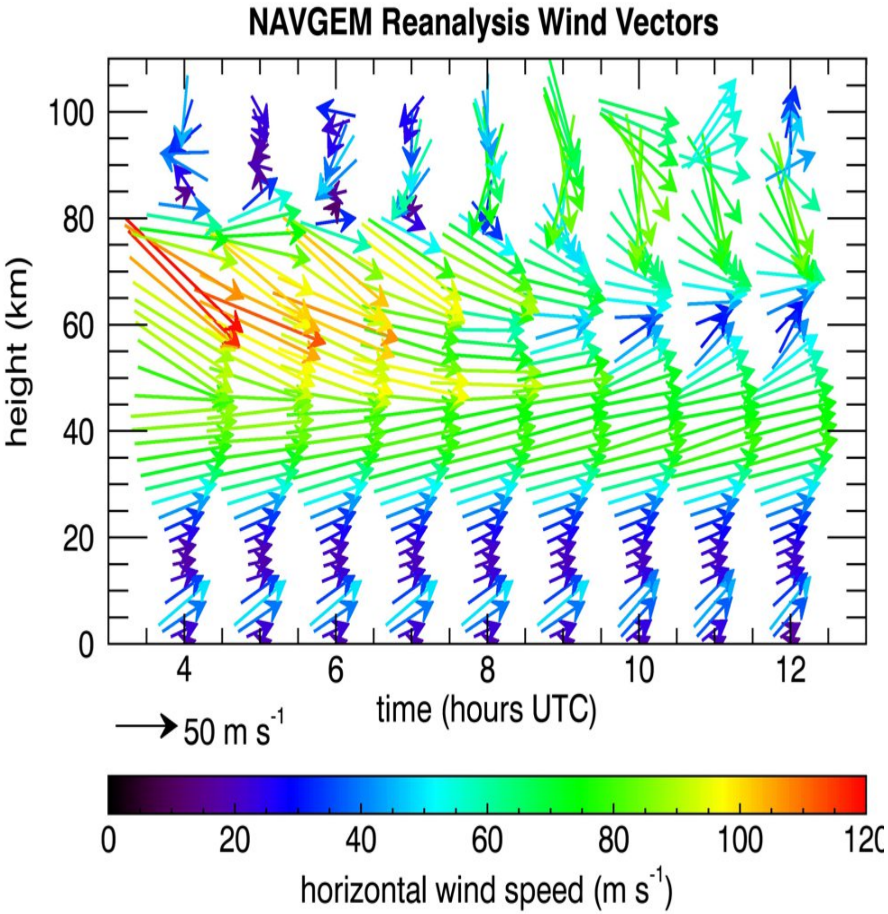

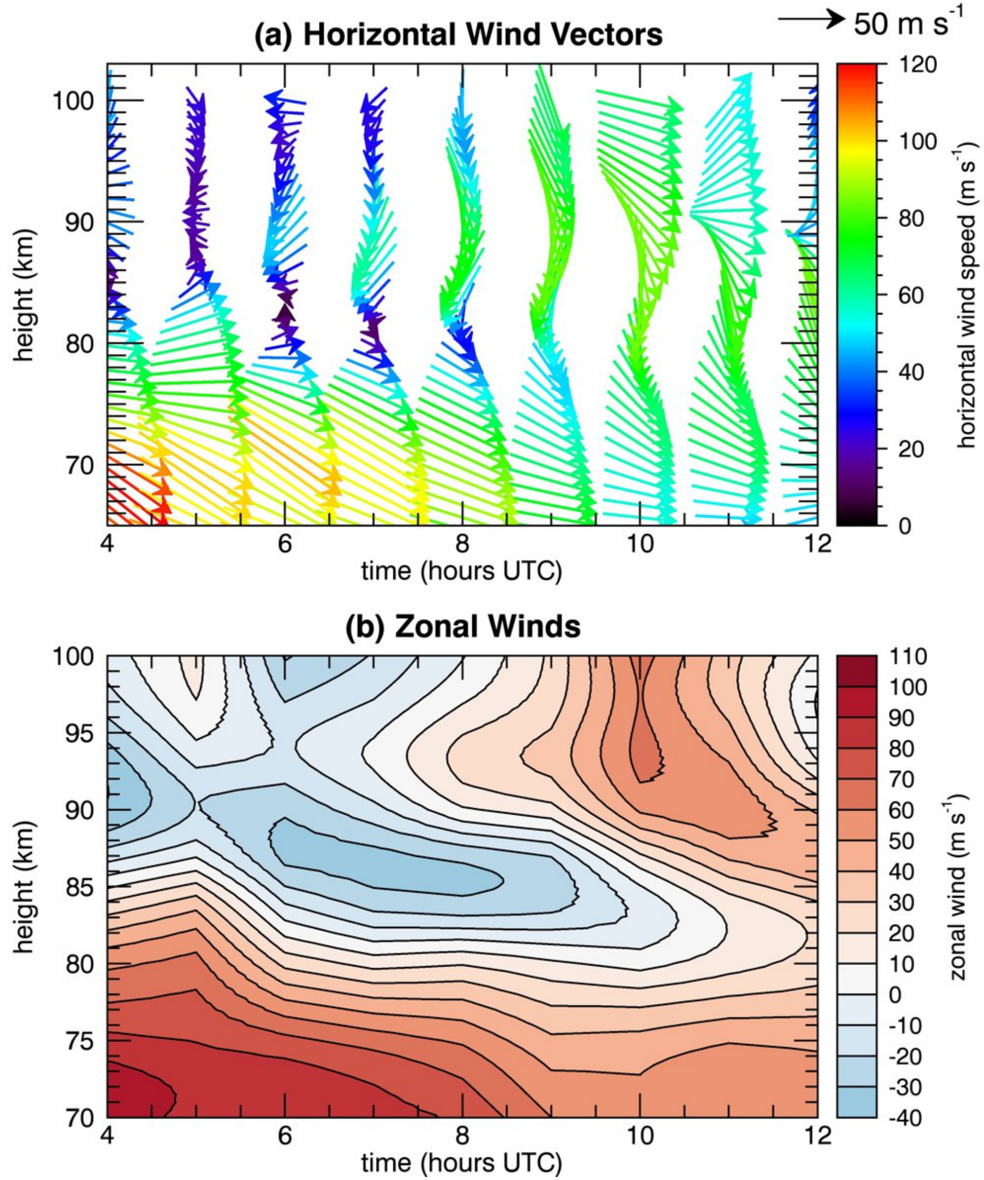

Large Migrating Semidiurnal Tide in MLT Reanalysis at 51°S

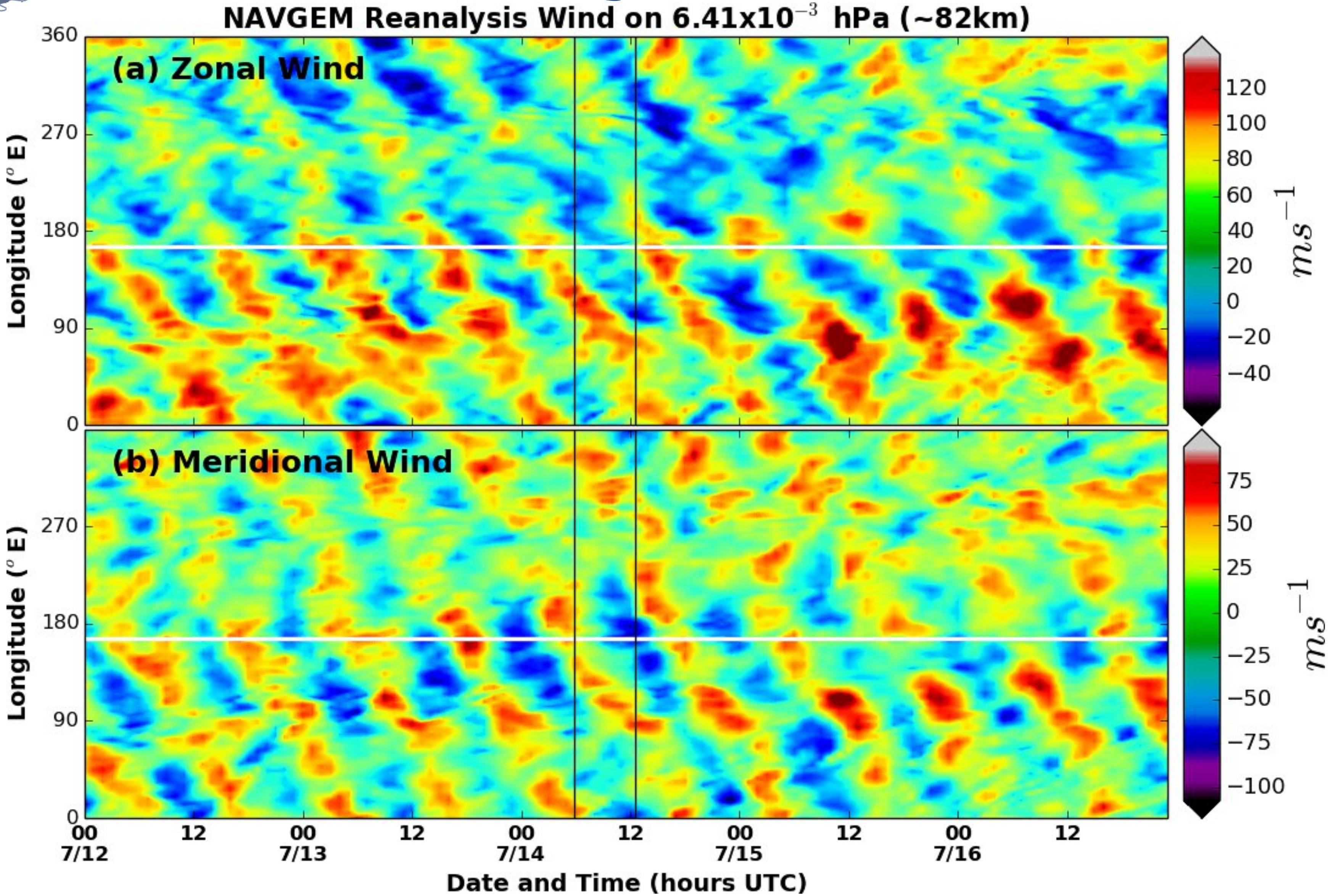

FR Modeled Breaking Heights

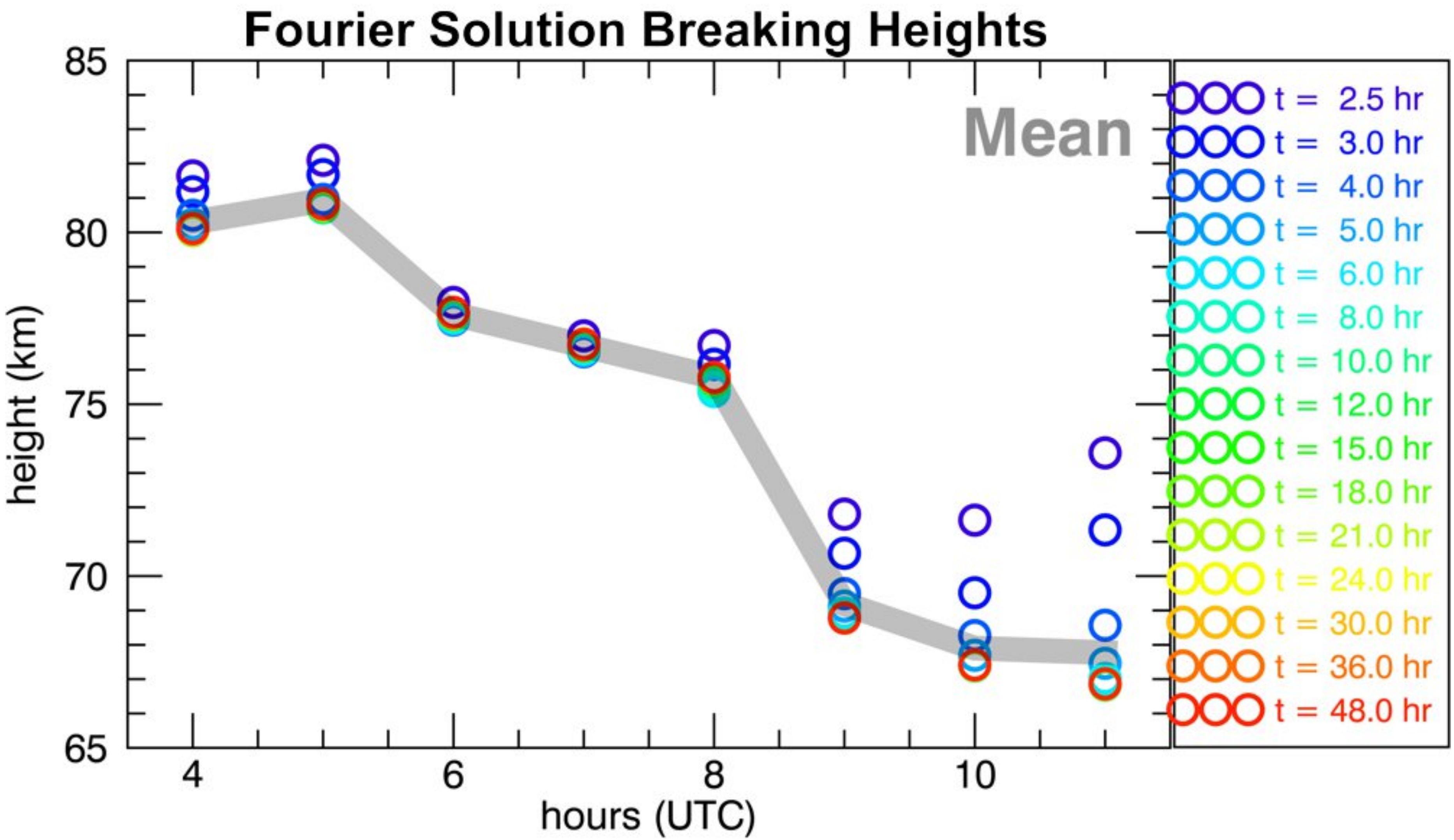

Time Evolution of Wavefields

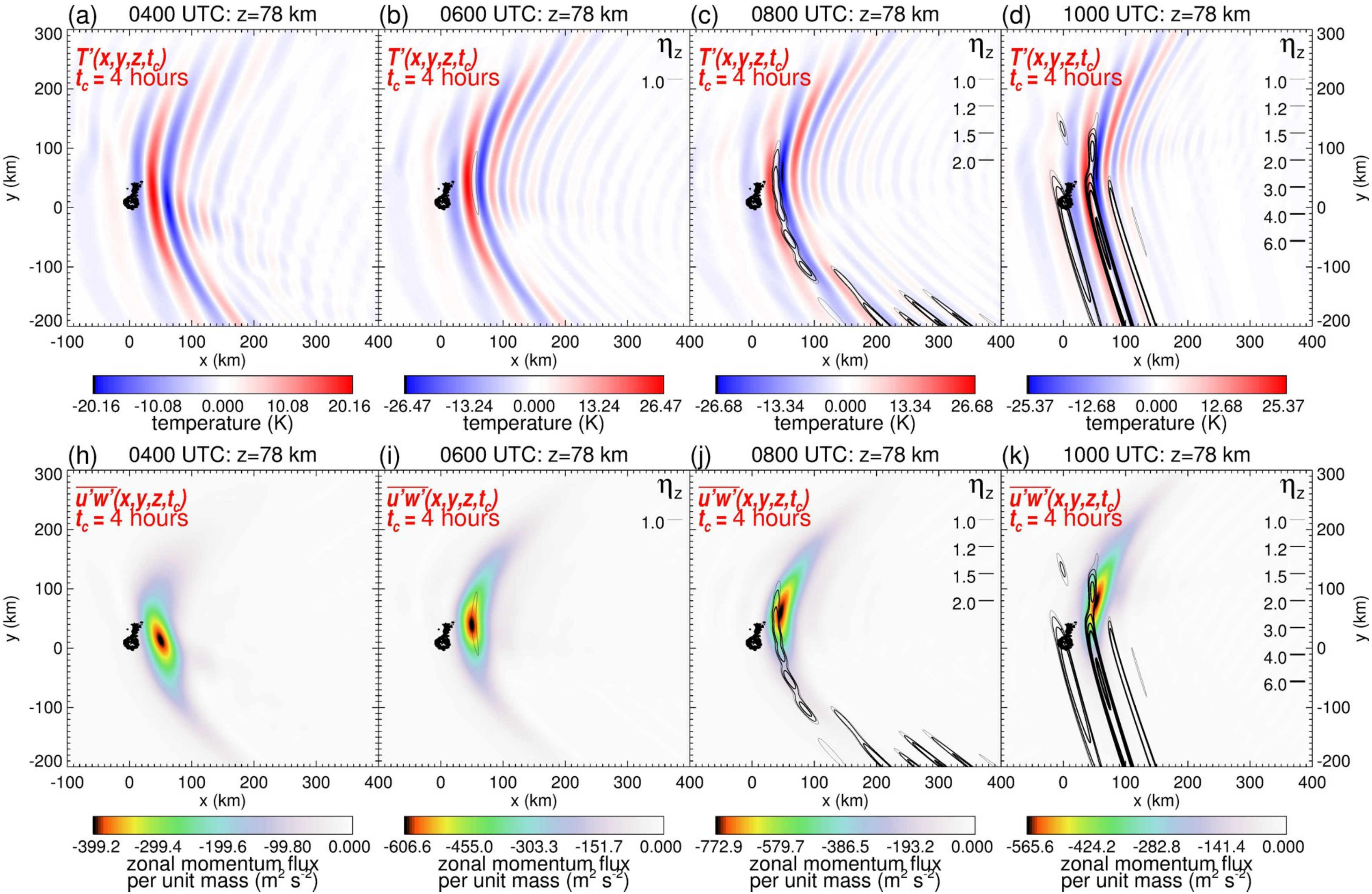

Huge MLT Driving Effects

- Offline calculation using linear saturation theory
- Layer-averaged mean flow accelerations ~-350 m s^{-1} $hour^{-1}$
- Layer-averaged dynamical heating rates ~ 8 K $hour^{-1}$

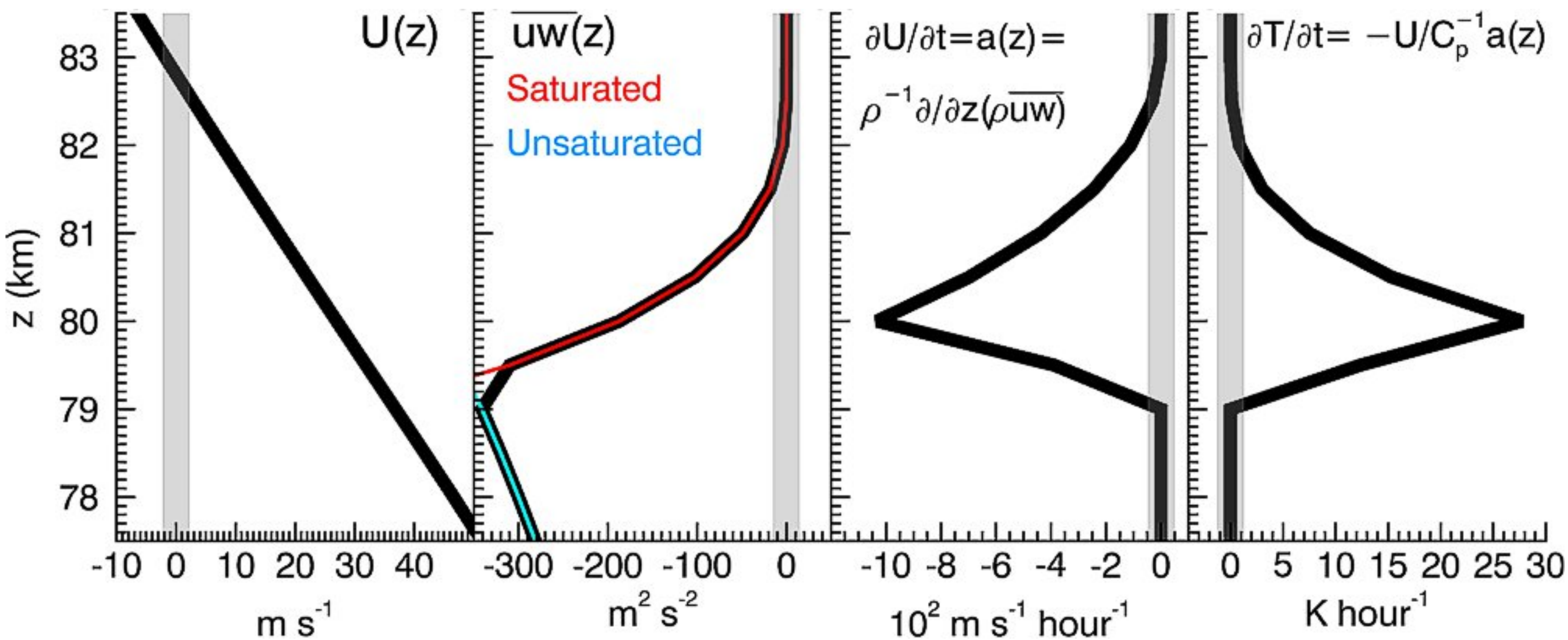

Conclusions

- RF23 supports important role of small subantarctic mountains to middle atmosphere momentum (and heat!) budget in austral winter (Alexander et al. 2009; McLandress et al. 2012; Alexander and Grimsdell, 2013)
- How does wavefield stay linear up to ~78 km before breaking?
  1. Spectral filtering of wavefield content (turning points & directional critical levels)
  2. Horizontal geometrical spreading of wavefields
  3. Nonhydrostatic downstream dispersion/spreading

  => Only nonhydrostatic solutions accurate: corresponding hydrostatic solutions are grossly inaccurate (parameterization implications)
- Huge MLT drag and heating rates (consistent with AMTM "warm up" in final overpass) with strong semidiurnal tidal modulation
- The "right" linear gravity-wave models <u>CAN</u> be accurate up to high altitudes right up to point of incipient wave breaking
- **see Eckermann et al., J. Atmos. Sci., submitted, 2016.**

BACKUP SLIDES

Model MLT Wavefields 0700 UTC

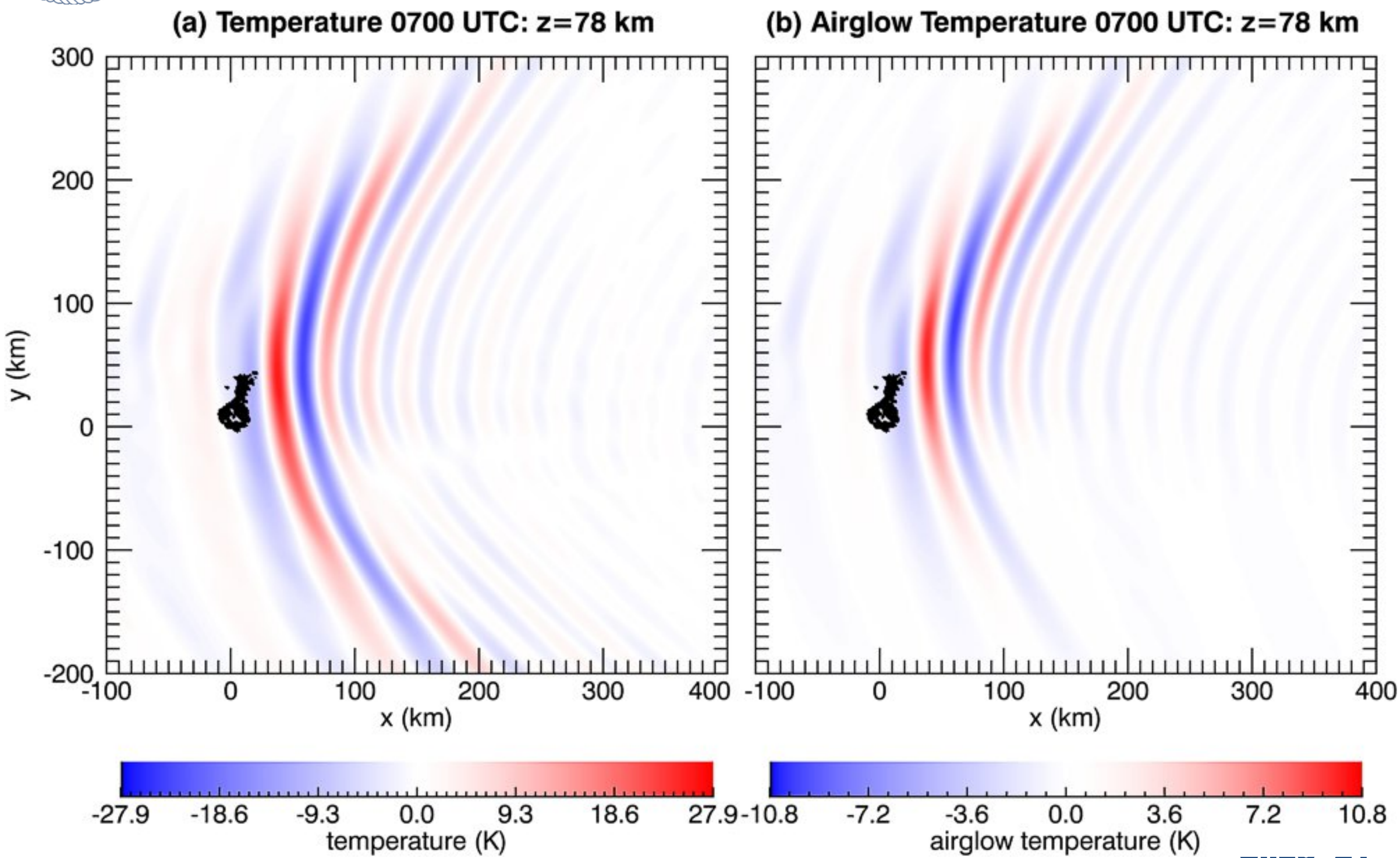

Inbound AMTM Imagery

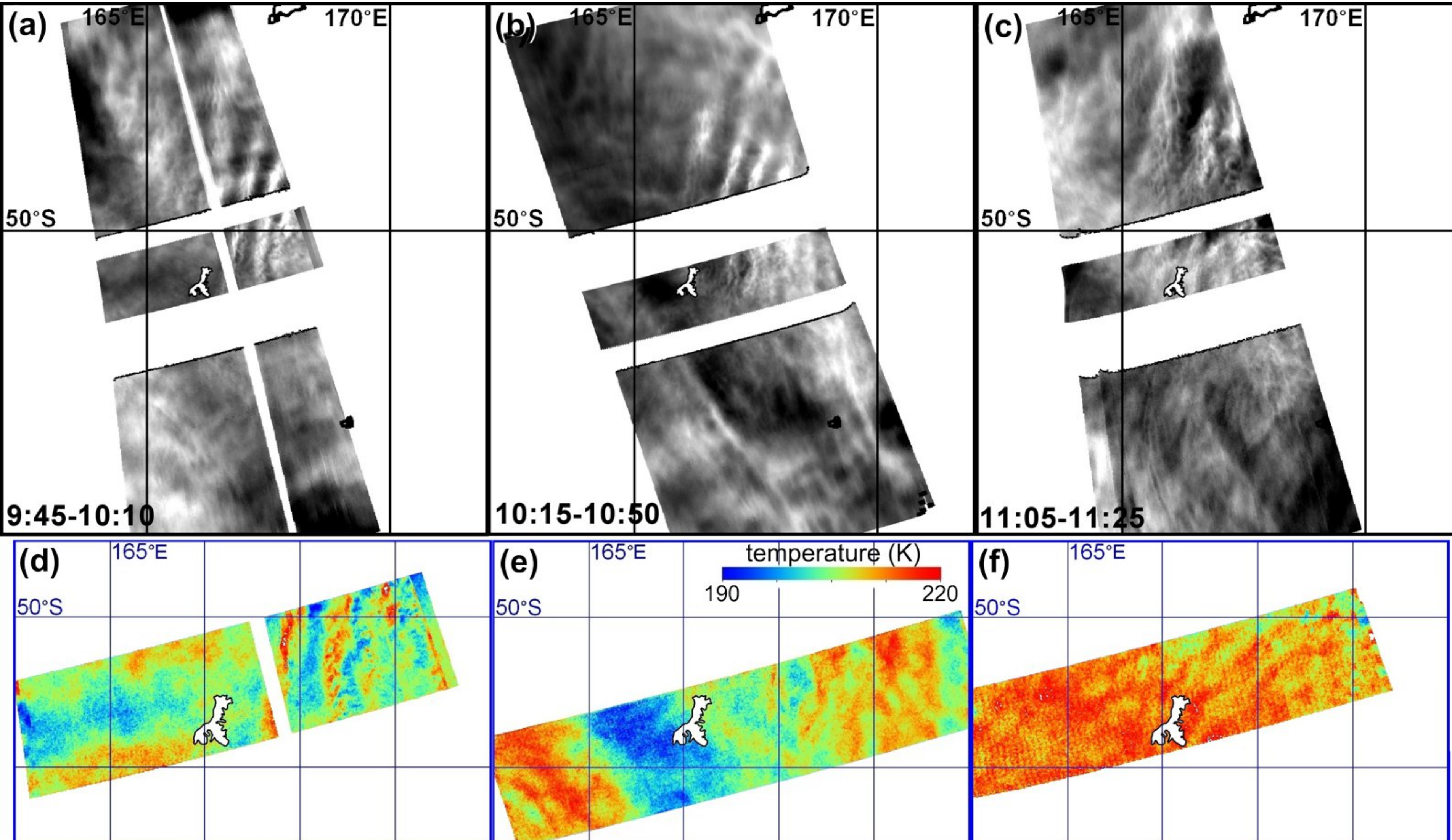

14 July 2014 0600 UTC: COAMPS 950 hPa

+18 hr Forecast

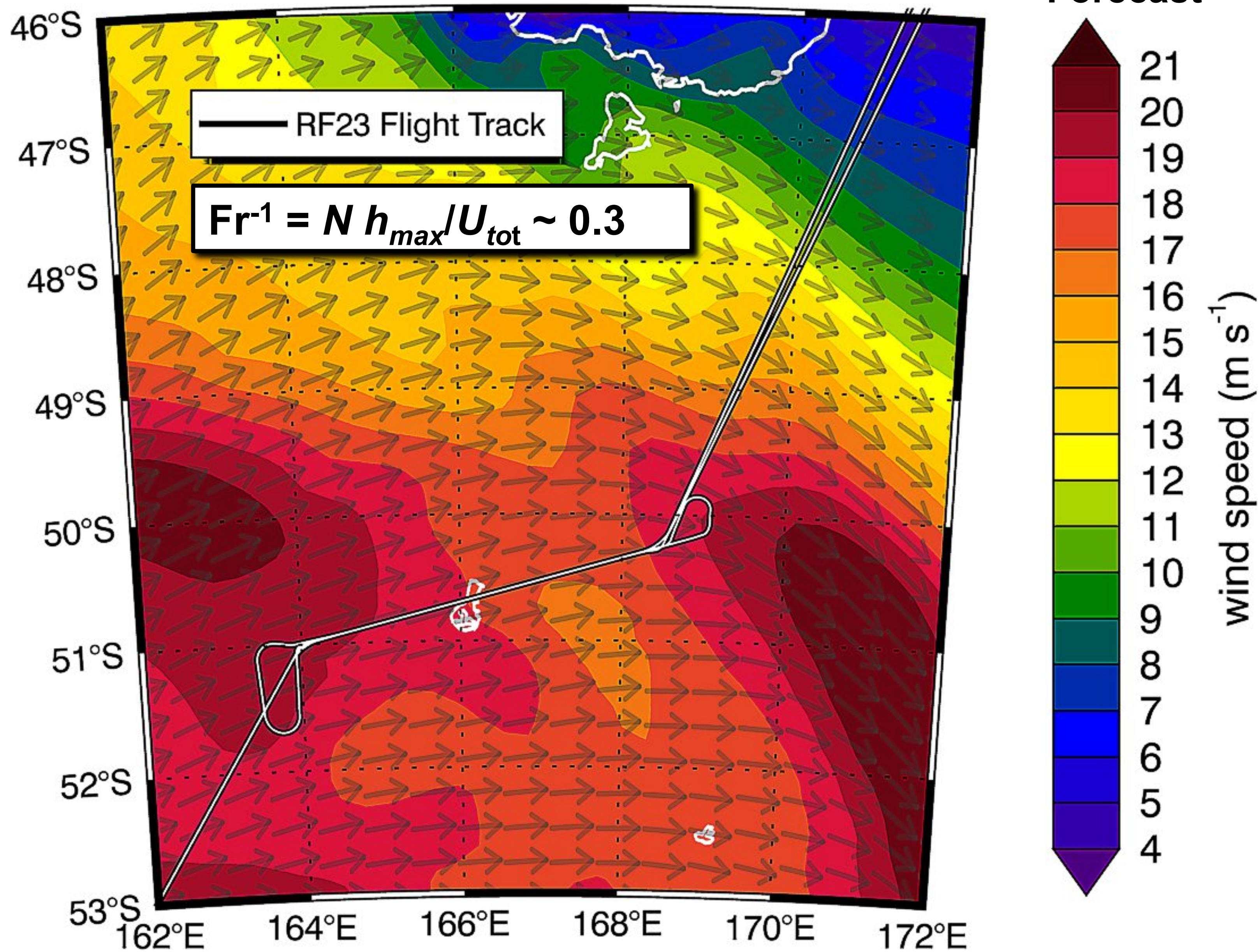

FR Model Momentum Fluxes

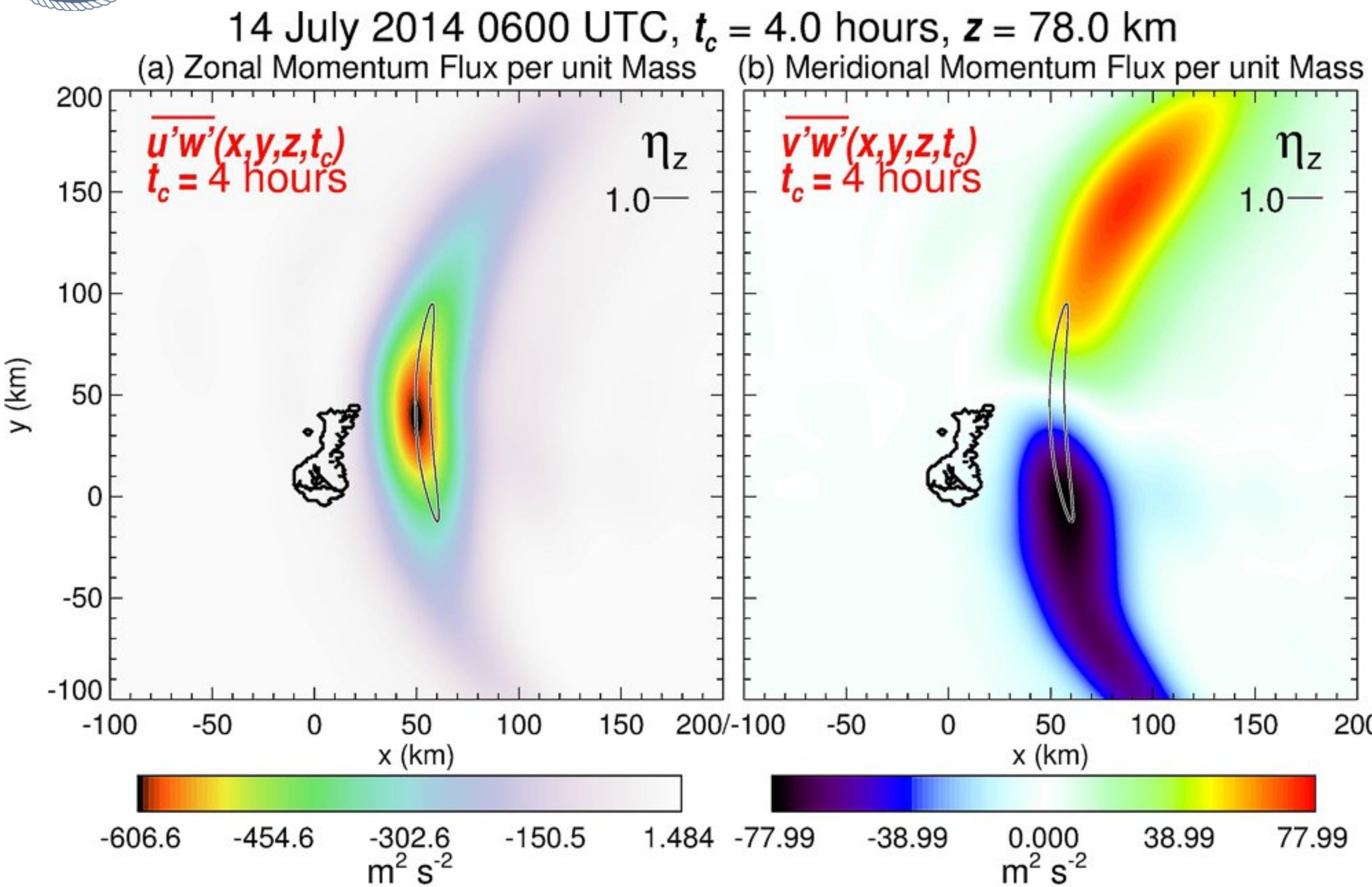

Model MLT Wavefields 1000 UTC

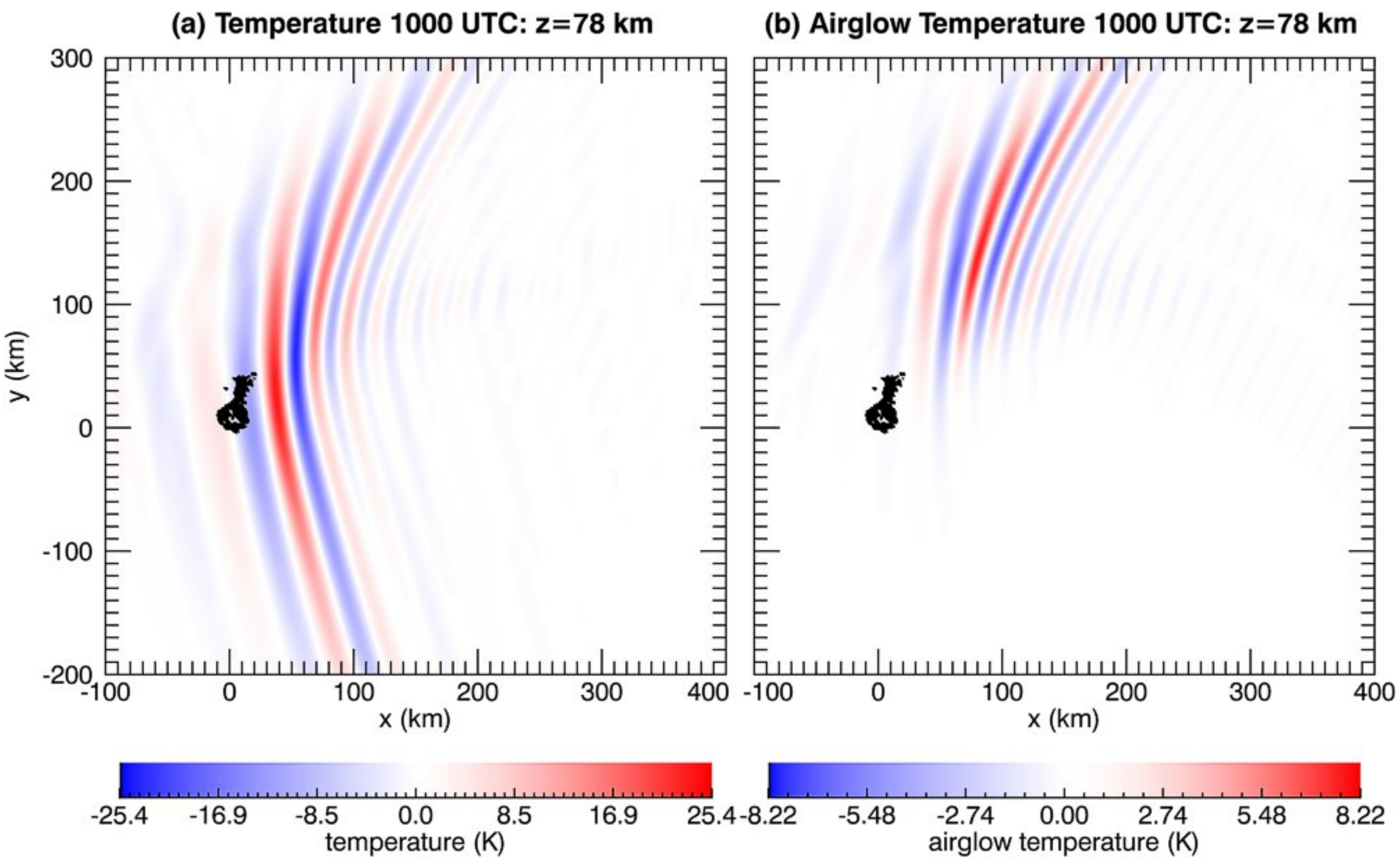

Linear Solution Approximations

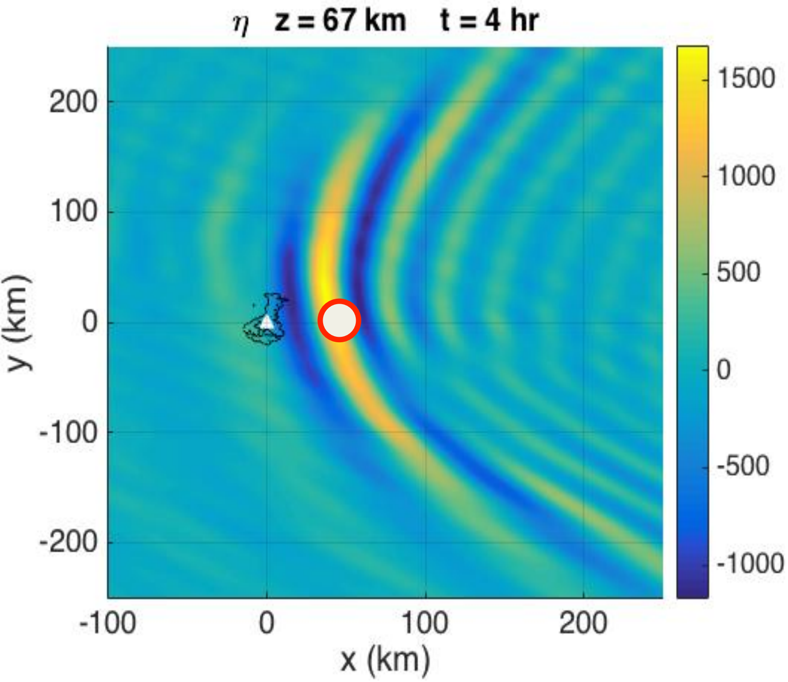

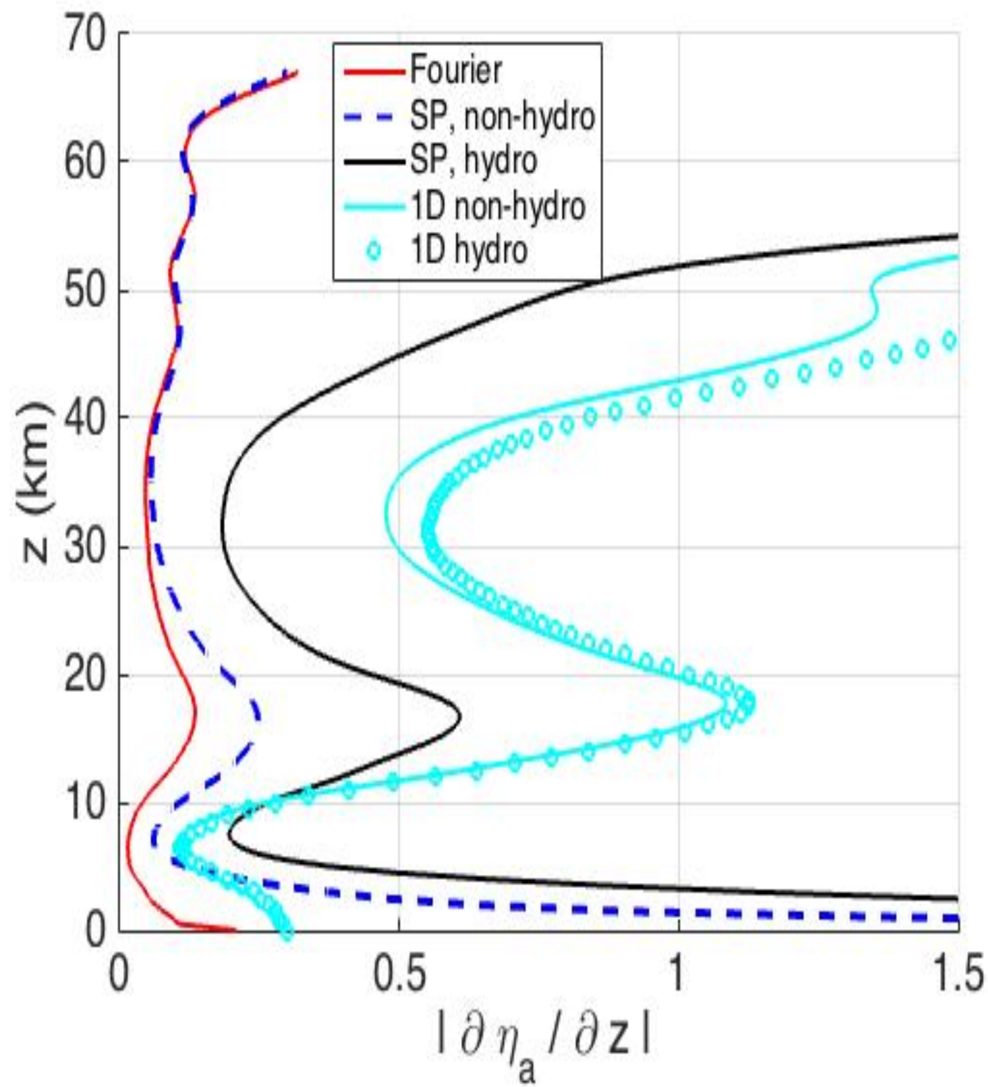

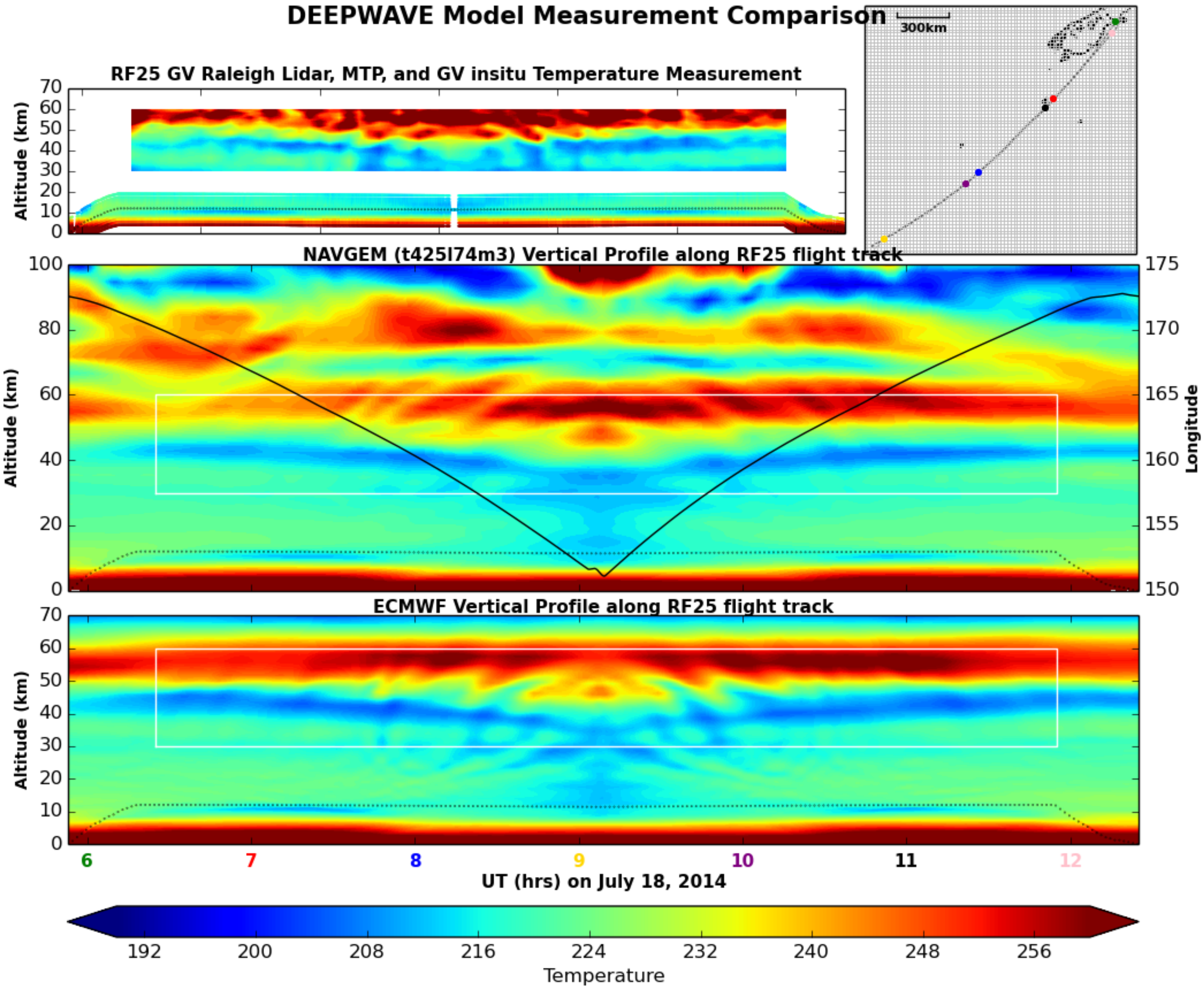

DEEPWAVE Model Measurement Comparison
300km
RF25 GV Raleigh Lidar, MTP, and GV insitu Temperature Measurement
Altitude (km)
NAVGEM (t425l74m3) Vertical Profile along RF25 flight track
Longitude
ECMWF Vertical Profile along RF25 flight track
6
7
8
9
10
11
12
UT (hrs) on July 18, 2014
192
200
208
216
224
232
240
248
256
Temperature

NAVGEM

Navy Global Environmental Model

Navy's bridge to a future ESPC

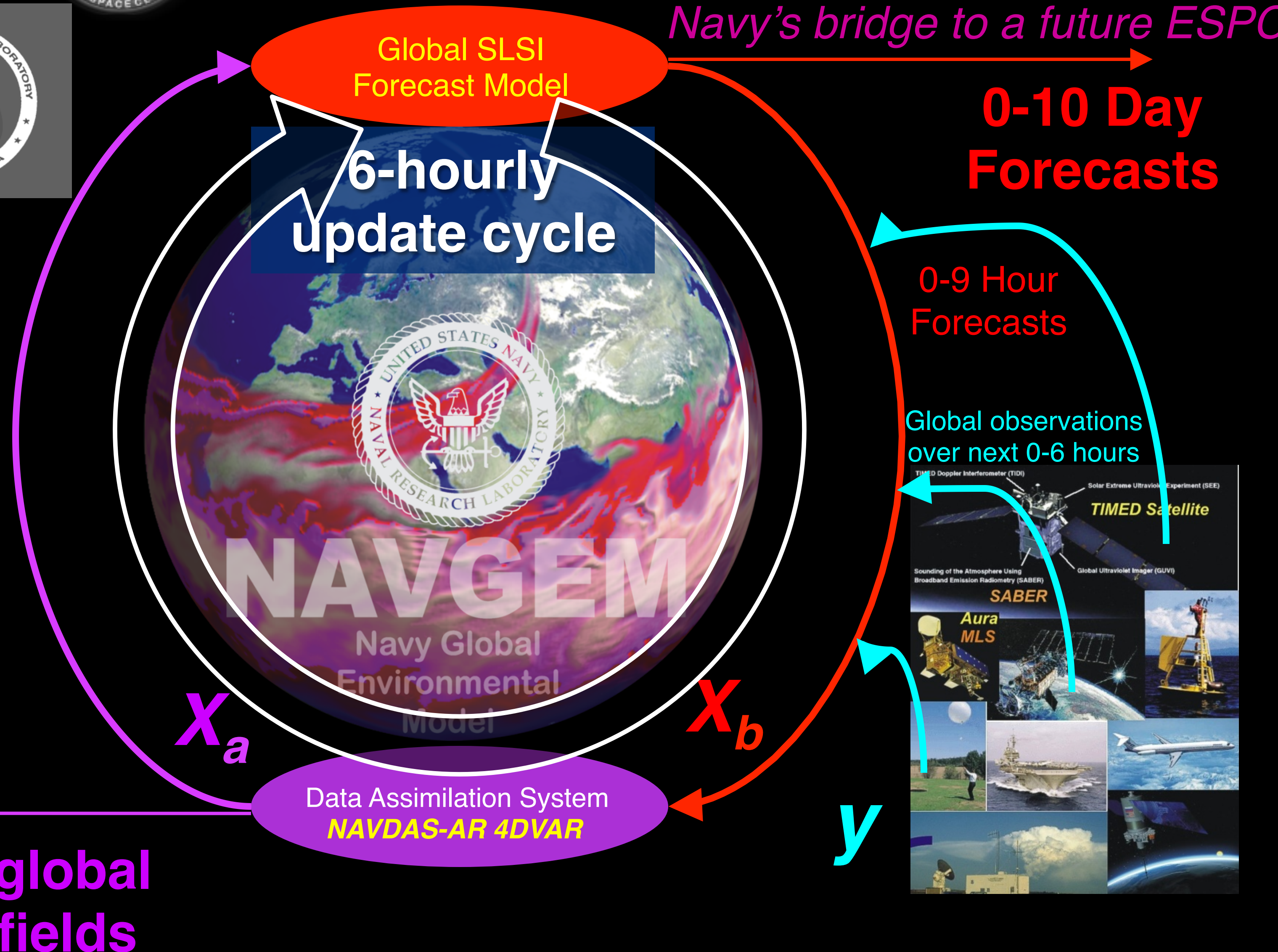

Hogan, T. F., M. Liu, J. A. Ridout, M. S. Peng, T. R. Whitcomb, B. C. Ruston, C. A. Reynolds, S. D. Eckermann, J. R. Moskaitis, N. L. Baker, J. P. McCormack, K. C. Viner, J. G. McLay, M. K. Flatau, L. Xu, C. Chen, and S. W. Chang (2014), The Navy Global Environmental Model, Oceanography, 27(3), 116-125, dx.doi.org/10.5670/oceanog.2014.73.

ATMOSPHEIC BACKGROUNDS:

NAVGEM 0-100 km Reanalysis for DEEPWAVE Austral Winter

Global Model Physics Modules Needed for Upper Levels

- Shortwave heating due to UV O_2 and O_3 photolysis
- Non-LTE CO_2 longwave cooling to space
- Exothermic Chemical Heating
- **Gravity-Wave Drag** (Momentum Deposition)
  - Orographic Sources of Gravity Wave Drag
  - Nonorographic Sources of Gravity Wave Drag
  - Frictional Heating (KE Dissipation)
  - Momentum/Heat Mixing due to GW-Induced Turbulence

The Deep Propagating Gravity Wave Experiment

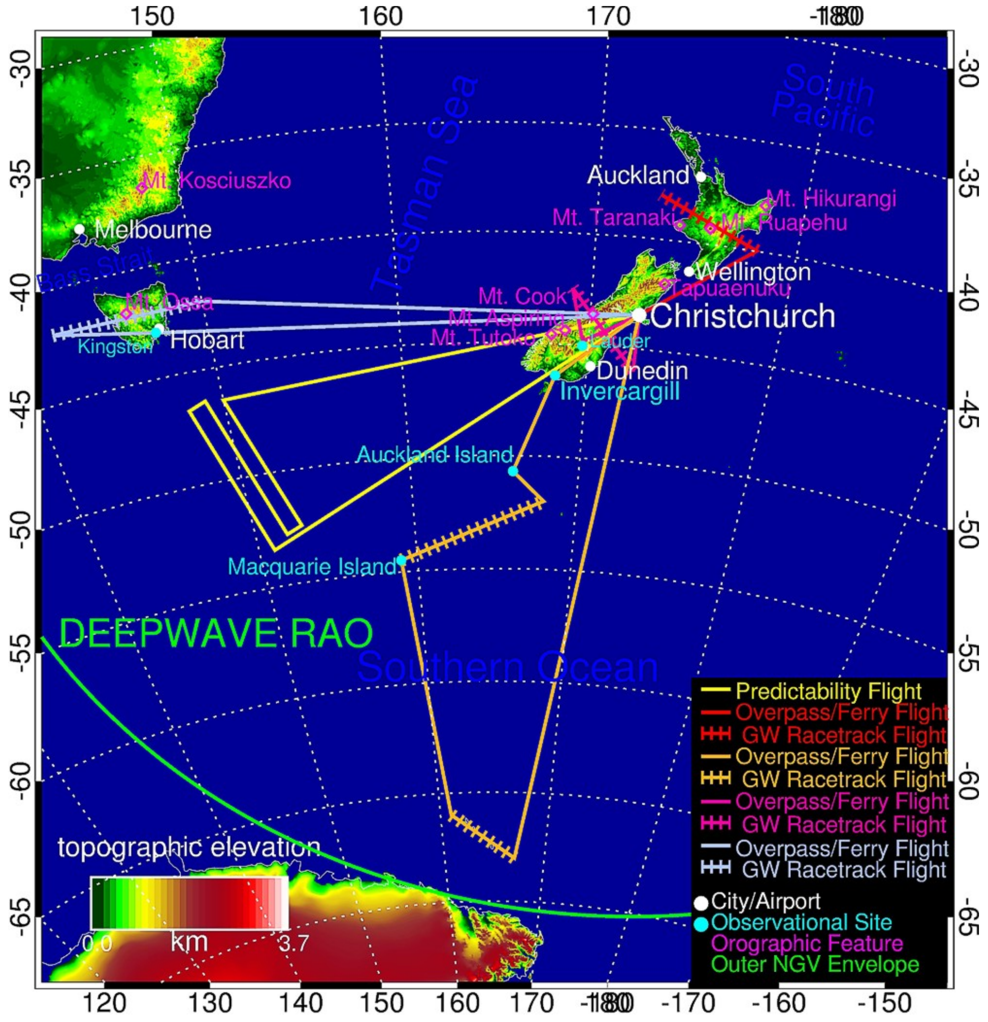

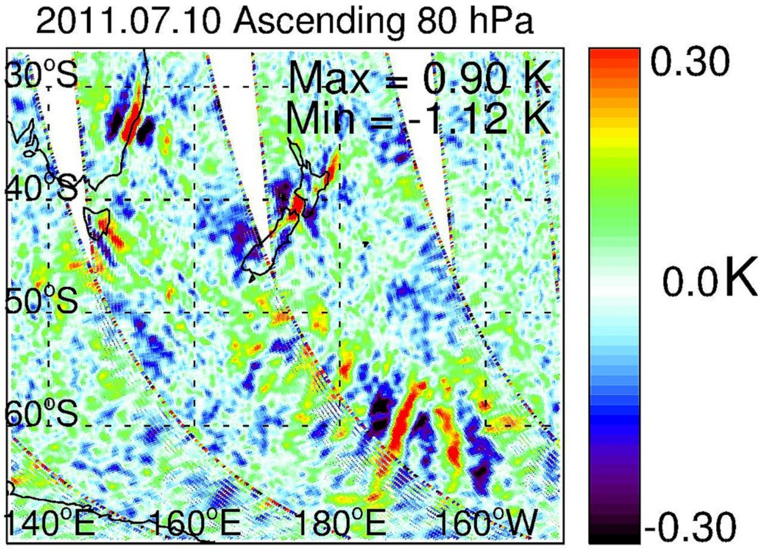

Climatological Winds vs. Height

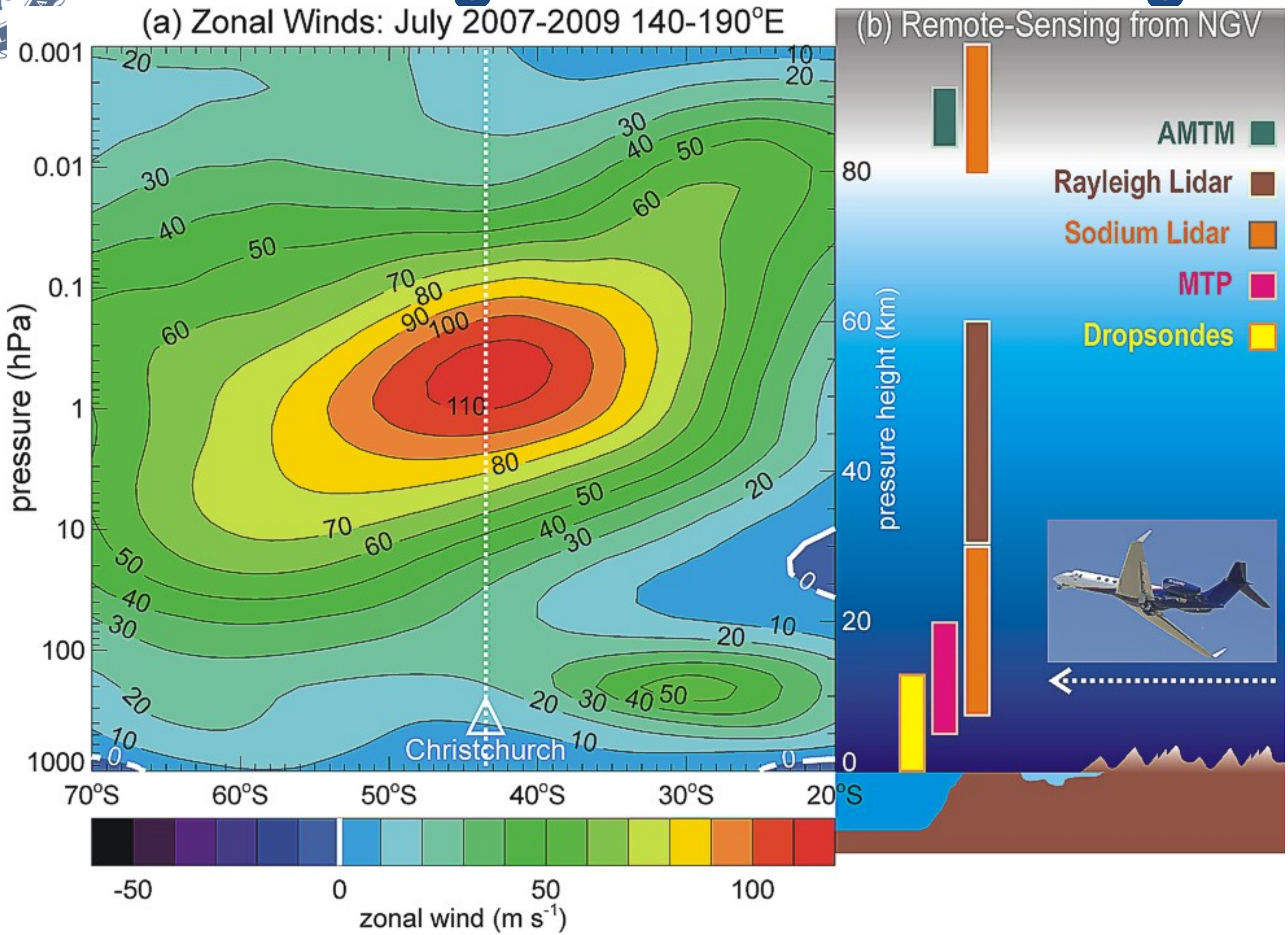

AIRS 7hPa RMS GW Radiances: 2002-2011

SAANGRIA

DEEPWAVE

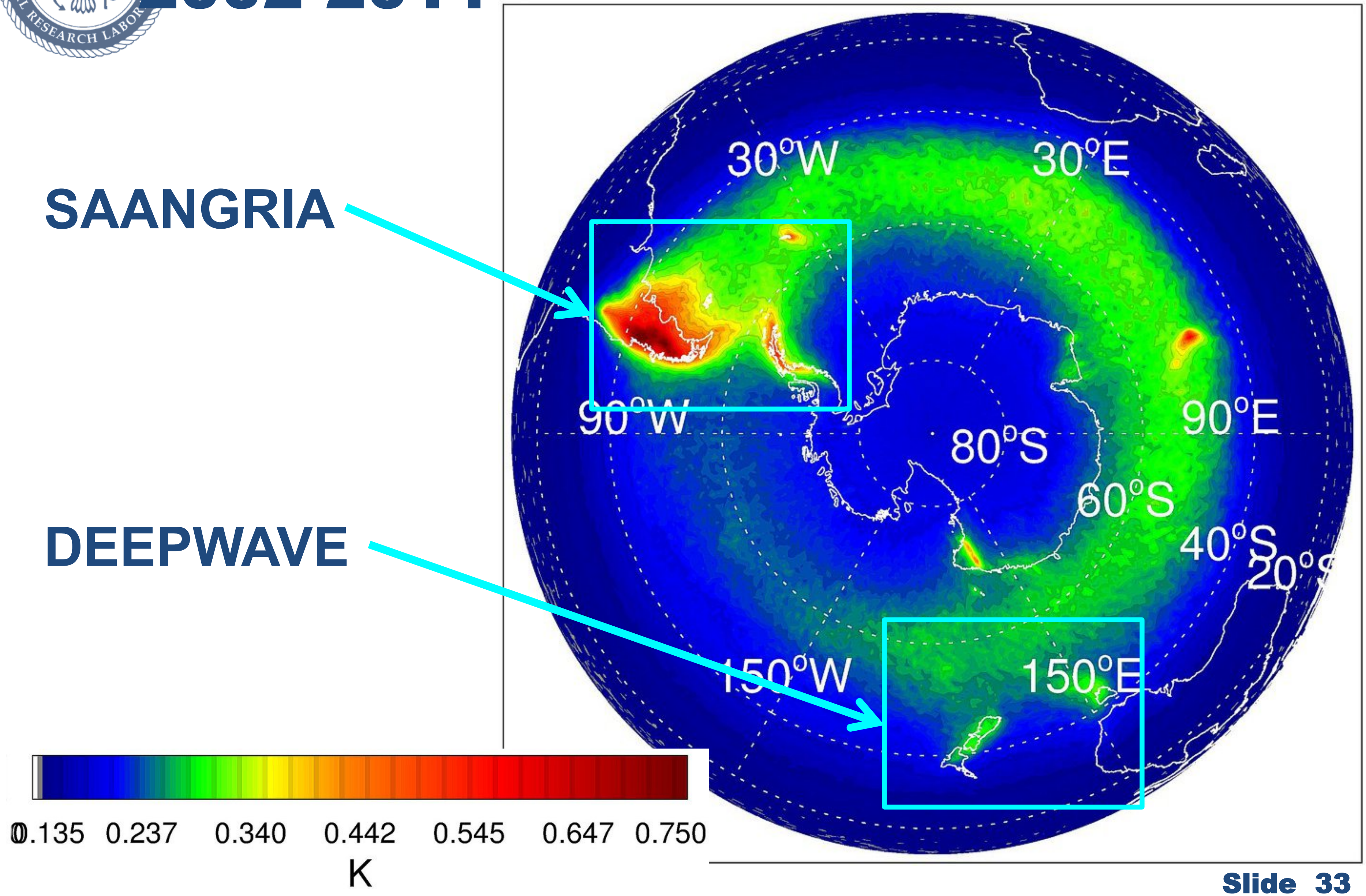

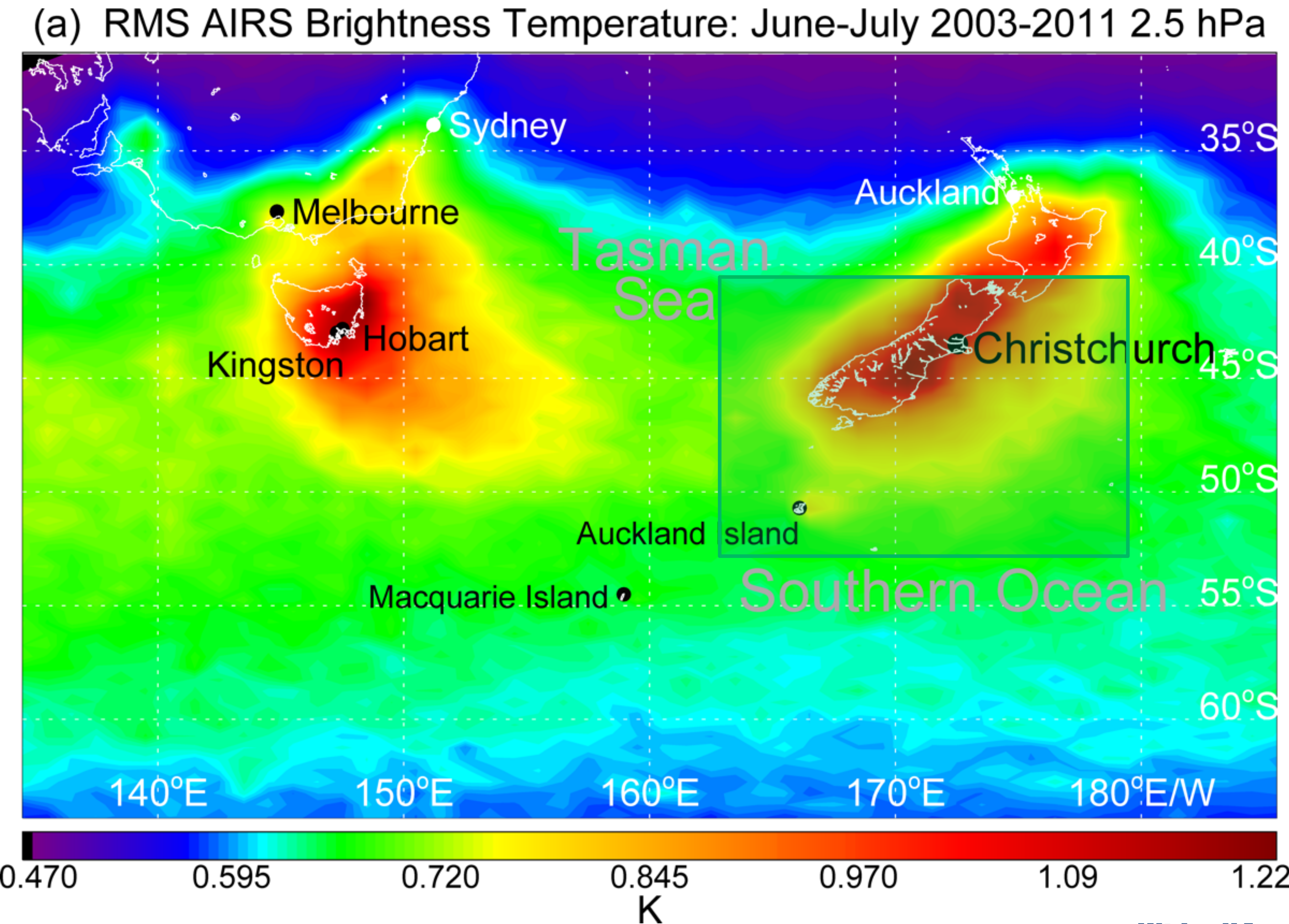
(a) RMS AIRS Brightness Temperature: June-July 2003-2011 2.5 hPa
Sydney
Melbourne
Tasman Sea
Auckland
Hobart
Kingston
Christchurch
Auckland Island
Macquarie Island
Southern Ocean
35°S
40°S
45°S
50°S
55°S
60°S
140°E
150°E
160°E
170°E
180°E/W
0.470
0.595
0.720
0.845
0.970
1.09
1.22
K

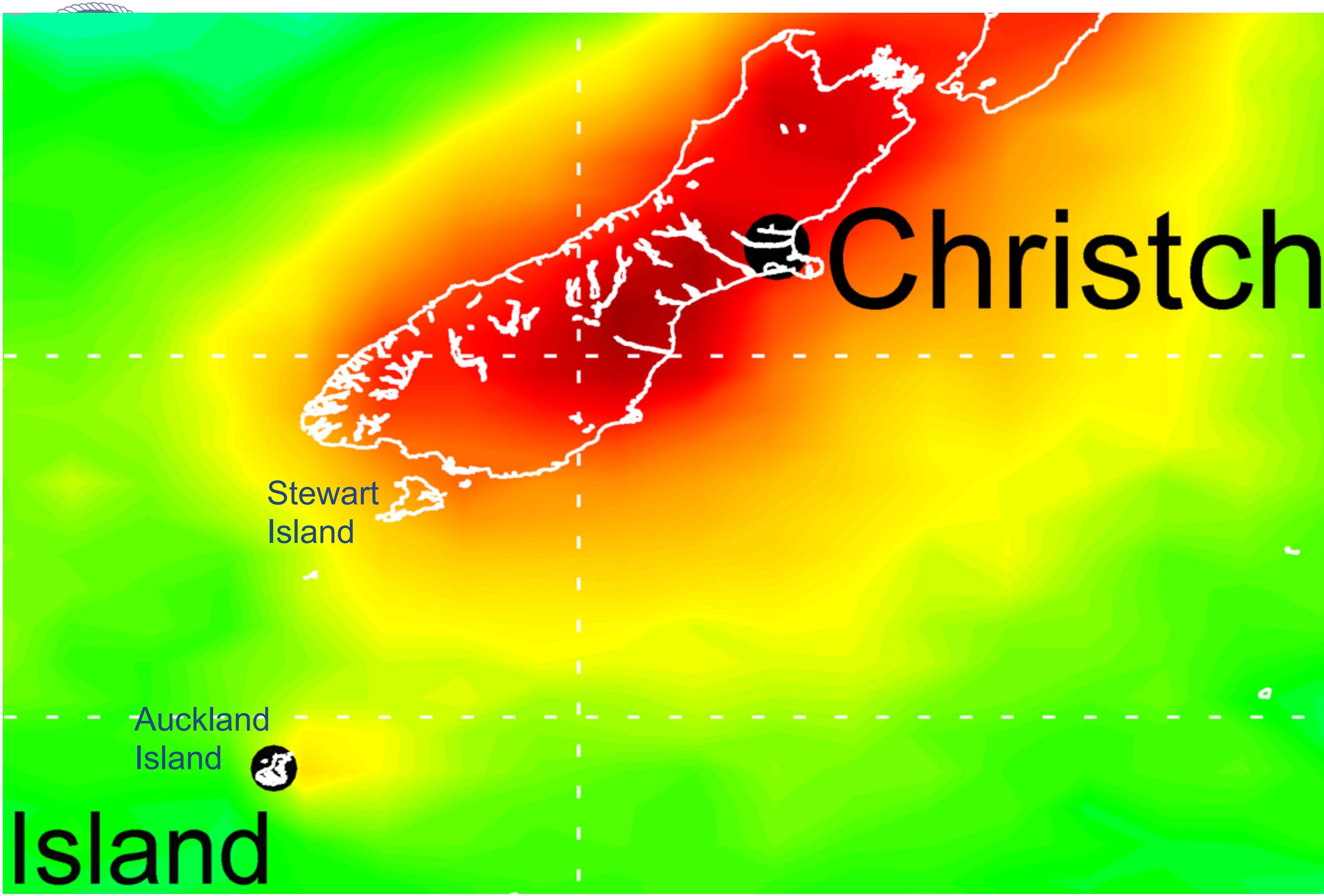

Christch
Stewart
Island
Auckland
Island
Island

DEEPWAVE Southern Climatology

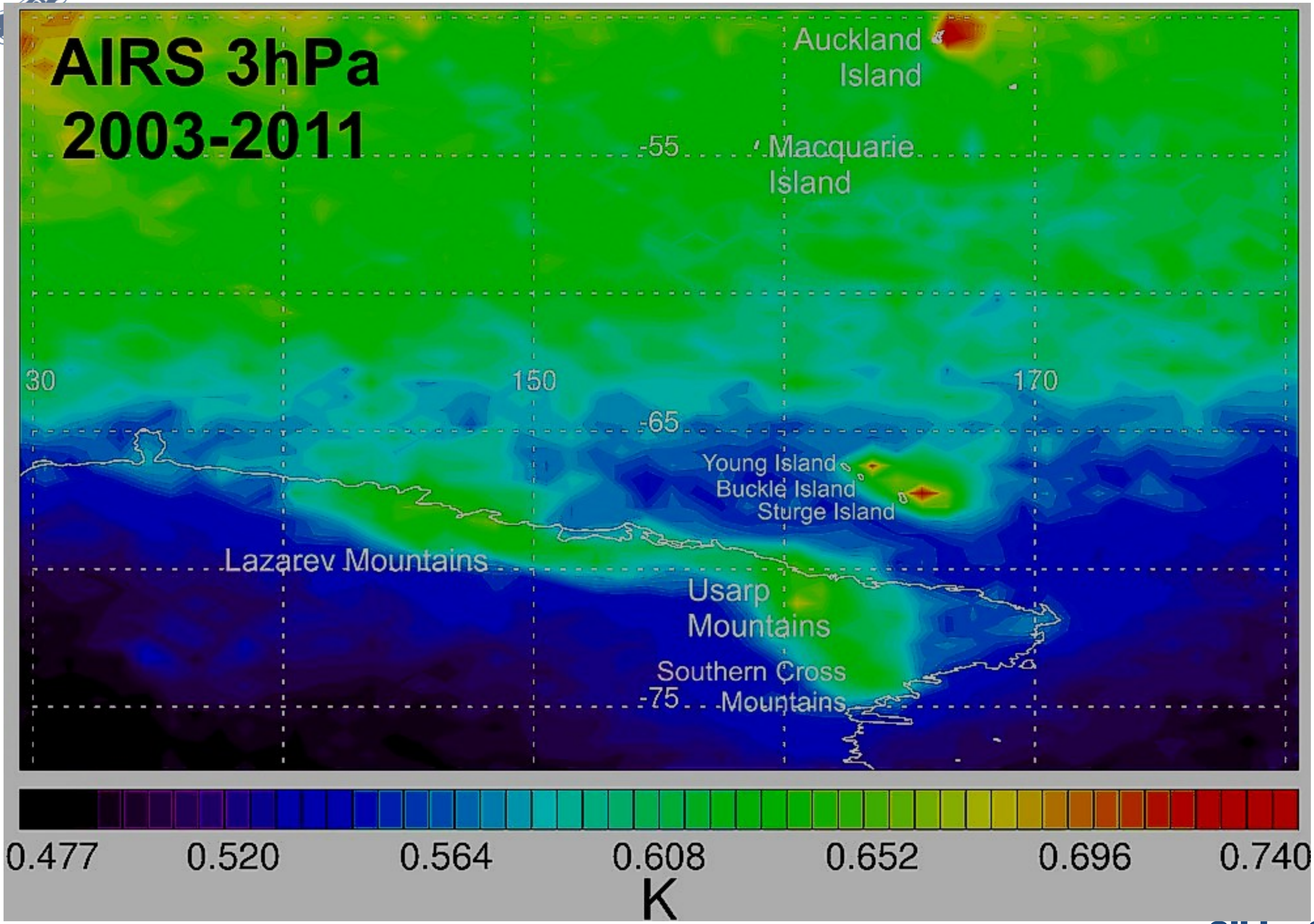

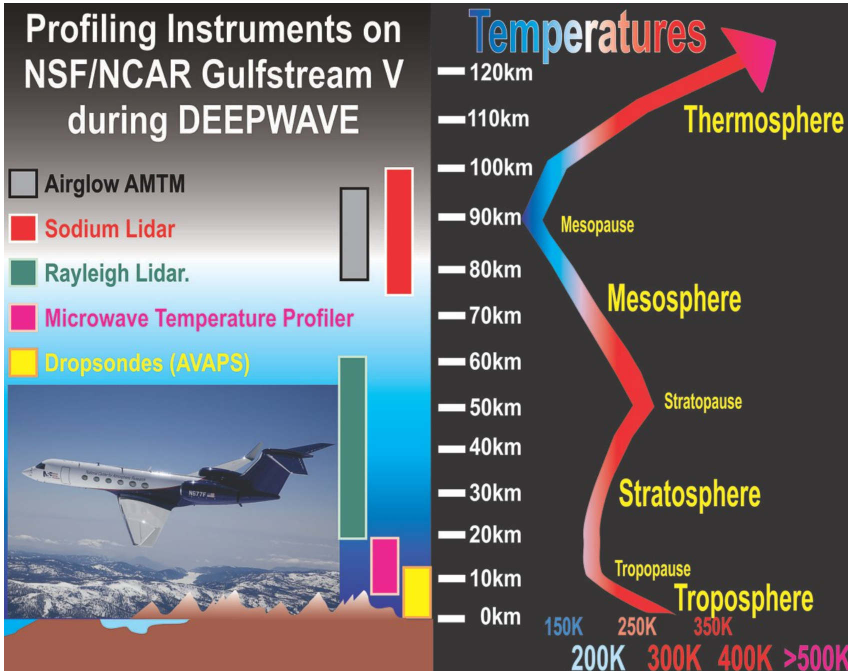

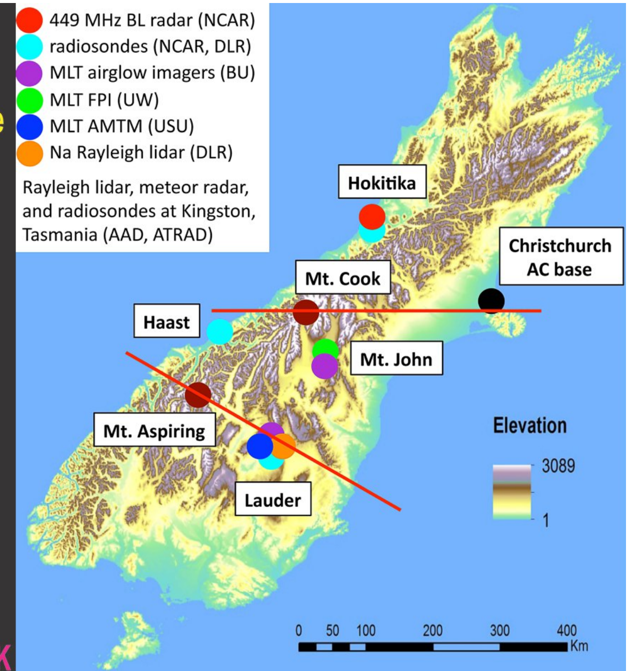

RMS AIRS Brightness Temperature: June-July 2003-2011 2.5 hPa

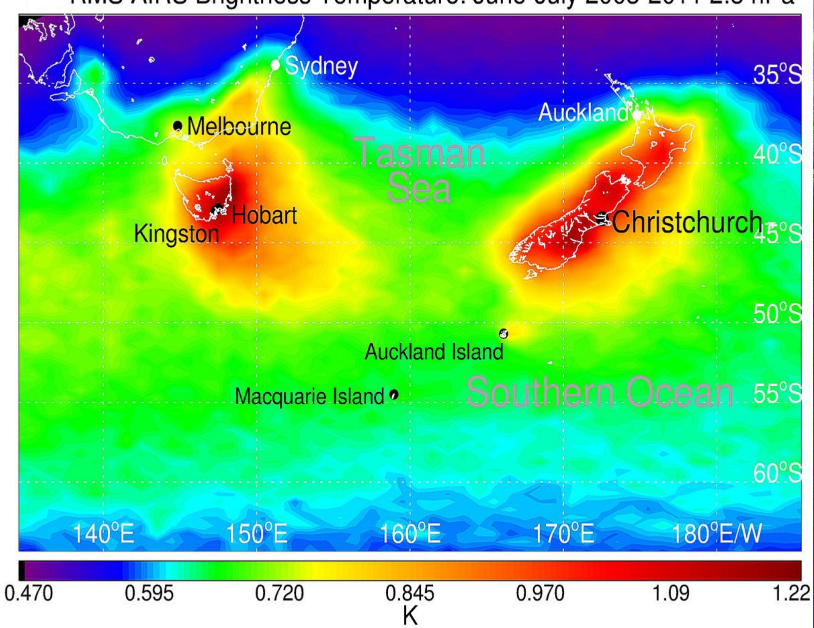

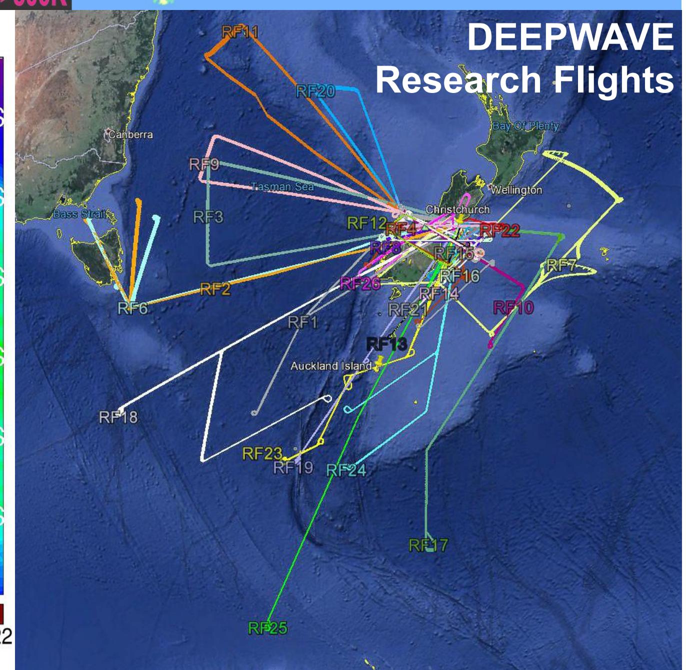

DEEPWAVE RF23

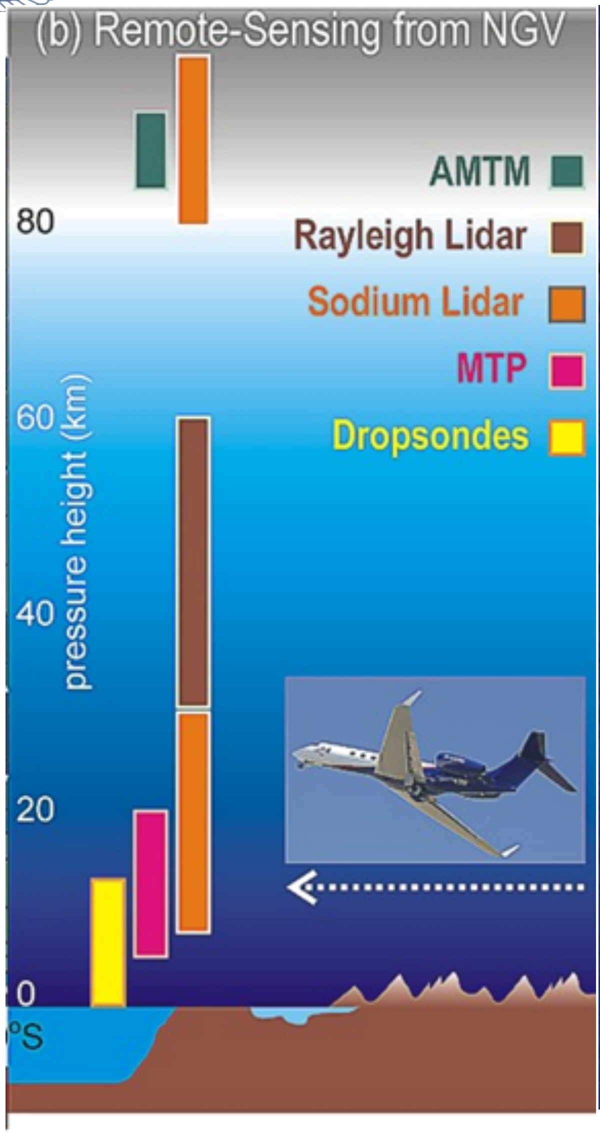

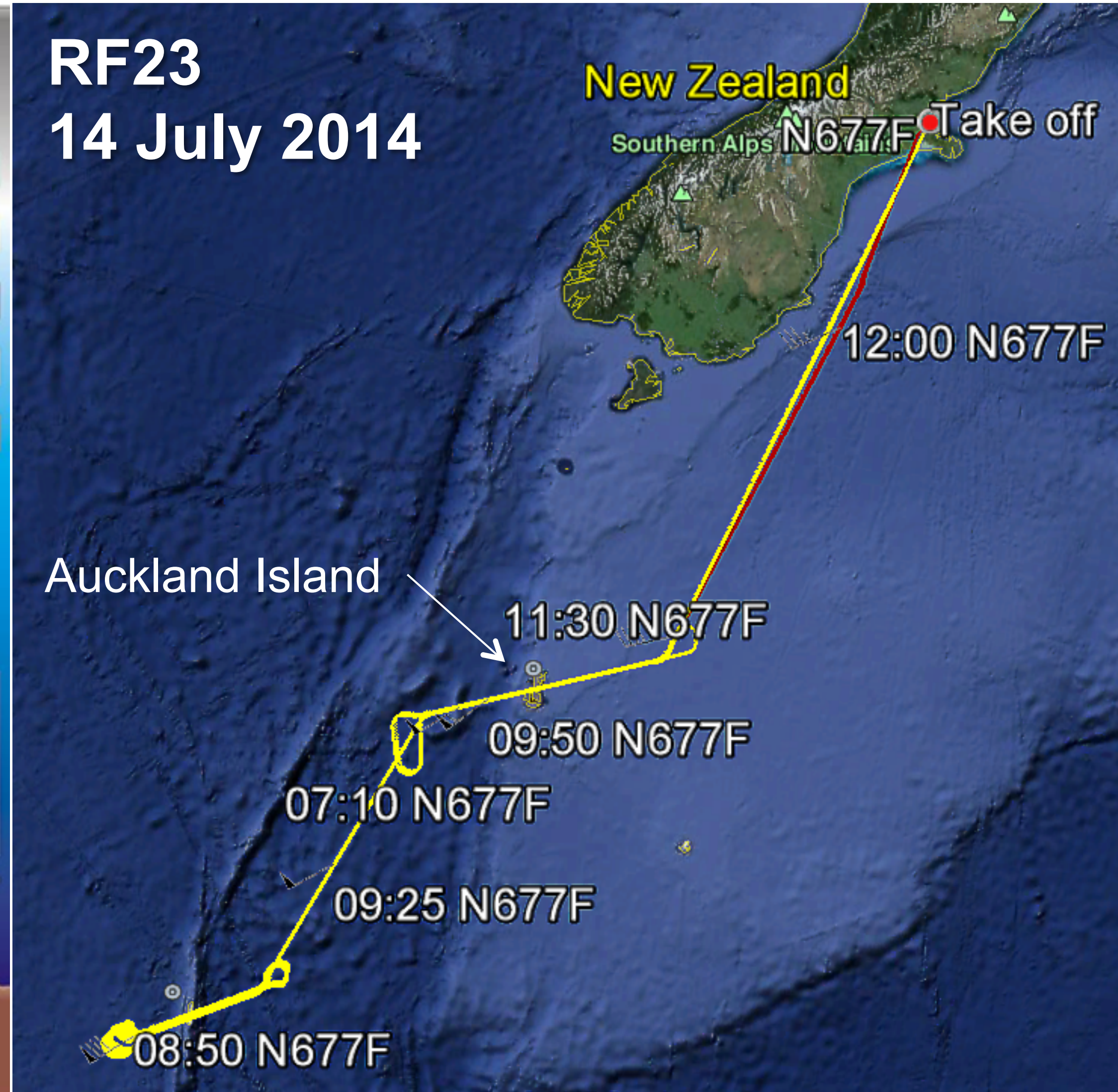

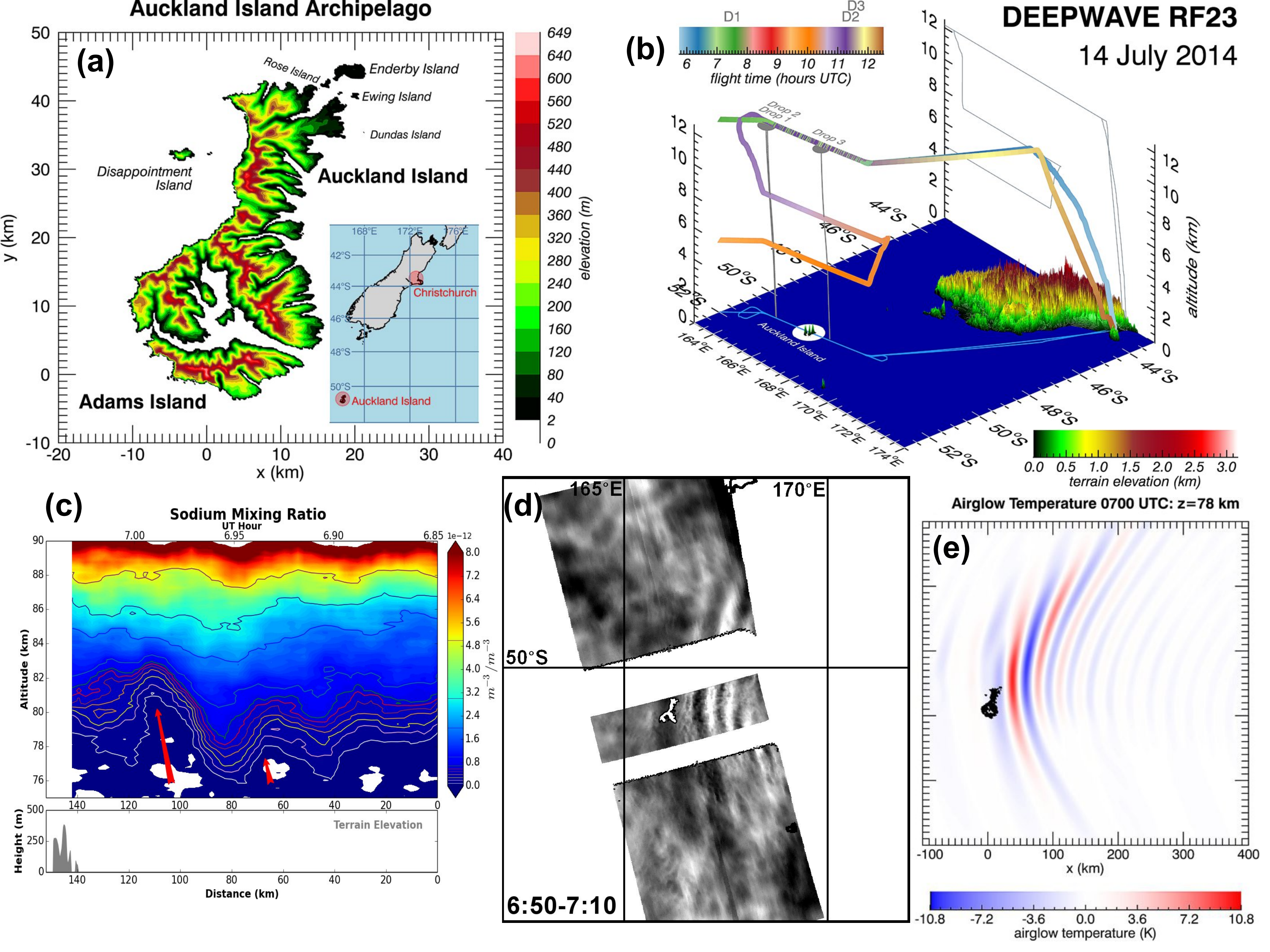

Auckland Island Archipelago
(a)
Rose Island
Enderby Island
Ewing Island
Dundas Island
Disappointment Island
Auckland Island
Adams Island
Christchurch
Auckland Island
elevation (m)
y (km)
x (km)
(b)
DEEPWAVE RF23
14 July 2014
D1
D2
D3
flight time (hours UTC)
Drop 2
Drop 1
Drop 3
Auckland Island
altitude (km)
terrain elevation (km)
(c)
Sodium Mixing Ratio
UT Hour
Altitude (km)
Terrain Elevation
Height (m)
Distance (km)
(d)
165°E
170°E
50°S
6:50-7:10
Airglow Temperature 0700 UTC: z=78 km
(e)
x (km)
airglow temperature (K)

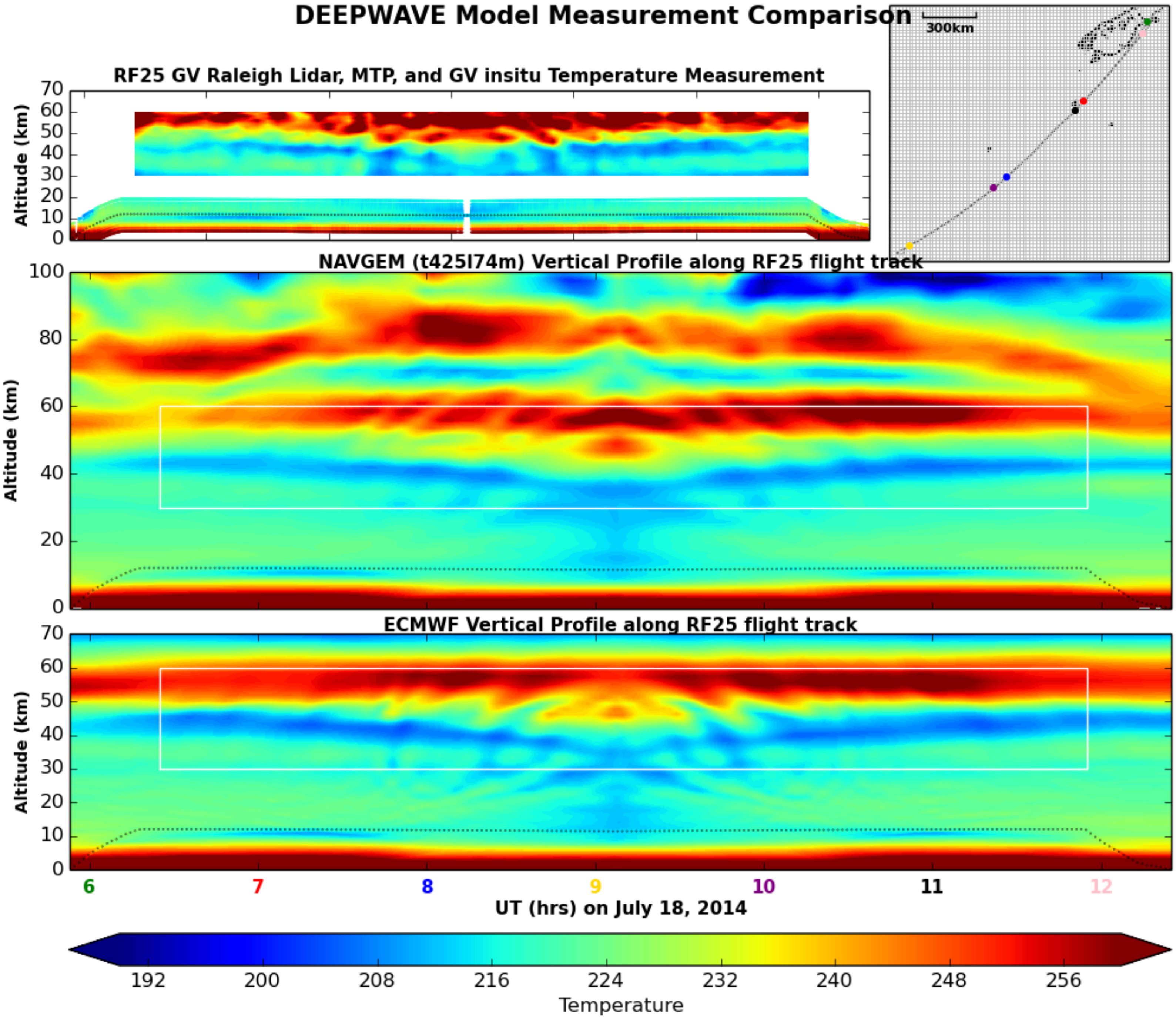

DEEPWAVE Model Measurement Comparison
300km
RF25 GV Raleigh Lidar, MTP, and GV insitu Temperature Measurement
Altitude (km)
NAVGEM (t425l74m) Vertical Profile along RF25 flight track
ECMWF Vertical Profile along RF25 flight track
6 7 8 9 10 11 12
UT (hrs) on July 18, 2014
192 200 208 216 224 232 240 248 256
Temperature